Spring 5-23-2019

Directional Comparison Bus Protection Using Superimposed Partial Operating Current Characteristics

Bishwas Baral
bbaral@uno.edu

Directional Comparison Bus Protection Using Superimposed Partial Operating Current Characteristics

A Thesis

Submitted to the Graduate Faculty of the
University of New Orleans
in partial fulfillment of the
requirements for the degree of

Master of Science
in
Engineering
Electrical Engineering

By

Bishwas Baral

B.E. Tribhuvan University, 2014

May, 2019

Acknowledgement

I sincerely acknowledge the support received from my research and academic adviser Dr. Ittiphong Leevognwat for his support throughout my graduate study and research.

I heartfully thank Dr. Parviz Rastgoufard for his valuable feedback and insight on my work.

I sincerely thank Dr. Ebrahim Amiri for his continuous support throughout my study at the school.

I would like to thank Monir Hossain for his continuous suggestion throughout my thesis.

I also thank UNO-Entergy Power and Energy Research Laboratory (PERL) for giving me an opportunity to research and give access to all the software needed.

Finally, I would like to thank my family and friends for their support and encouragement.

Contents

List of Figures

List of Tables

Abstract

Various directional comparison bus protection methods including widely used superimposed directional element method need to have both voltages and currents from all feeders connected to the zone of protection to find the direction of current for detecting a bus fault or a line fault. The purpose of the thesis is to present a new technique for directional comparison bus protection to discriminate a bus fault from line fault and normal condition. The new technique, which is implementing superimposed directional element method to modify partial operating current characteristics (POC) method to superimposed POC (SPOC) method, does not use voltages from feeders, hence capacitor voltage transformers (CVTs) are no longer needed in the zone of protection. POC method needs to exclude load terminal current to detect fault during high impedance fault but the proposed technique does not need to exclude such currents. The proposed technique was implemented in 4-bus and IEEE 14-bus test system and was tested using different fault cases including CT saturation and high impedance fault. The proposed technique, SPOC method was compared with POC method with both methods implemented in same test systems and tested with same fault cases. The results show that the proposed technique is successful to detect bus faults with high accuracy and high speed.

Keywords: EMTP, MATLAB, 4-bus system, IEEE 14-bus system, Direction Protection, Steady State, Faults.

Chapter 1
Introduction

This chapter provides an overview of power systems and its protection. Different protection in power systems including bus protection is explained in section 1.1. Literature review of bus protection with widely used methods of bus protection is explained in section 1.2. Finally, section 1.3 explains the scope and contribution of the thesis in directional comparison bus protection.

1.1 Power System and Its Protection

A power system is the combination of electrical components that are used to supply, transfer and use electrical power. It contains complex elements such as a generator, buses, transmission lines, transformers, and loads. In this complex system, faults may occur and affect the flow of electrical power and damage power systems equipment. A fault is a failure that interferes with the normal flow of current because it provides a low impedance path. The primary goal of any electrical utility is to supply uninterrupted power to end consumers. To achieve this a power system needs to have a good protection system. The main purpose of power systems protection is to detect and isolate the faulty section so that the rest of the system operates without any severe damage to equipment such as generators, transformers, bus bars, and overhead transmission lines because of the fault. Circuit breakers (CB) and relays are the main components for any power system protection scheme. A protective relay is a microprocessor-based device that takes an input of currents and voltages from current

transformers (CTs) and voltage transformers (CVTs), detects the abnormality, and gives control signal to CB. A CB after receiving a trip signal from the relay then isolates the fault from the rest of the system by tripping the faulted section during an abnormal condition [1]. A current transformer (CT) changes the high magnitude of primary current to lower magnitude in its secondary. CT is an important component because it is used for current measurement that is used by a relay to monitor and protect power systems. All the CTs have burden associated with them. CT burden is the external load that is applied to the secondary of a CT. The burden is largely a resistive and inductive load. The performance of CT during normal operation of the system and during a fault affects the performance of the relay. When CT operates under normal operation, CT output is the same to its primary current input adjusted by CT ratio. But during a fault, CT output is drastically affected as the CT saturates because of CT burden combined with high primary fault current. The effect of CT saturation on fault detection is explained further in the next section.

A protection scheme has several important functional requirements to disconnect the faulty section. Reliability is one of the important requirements of a protection scheme. The relays should remain idle and inoperative for a long time and should be able to respond instantly when a fault occurs. The speed of operation is another important requirement of power system protection. The protection relays should operate within a set time duration after the fault.

Each type of power system component like generators, transmission lines, transformers, and buses usually has its own protection. This thesis is focused on bus protection by tripping the bus for faults on the bus and not tripping for faults outside the bus. Faults on a bus are rare but occurrence may cause major shutdown as a bus is the connection point of

many electrical components like generators, transmission lines, and loads as seen in Fig [1.1]. Therefore, a bus protection method should be of high integrity [2]. Similar to any protection method, bus protection method should remain idle and inoperative for a long time but should respond instantly when fault occurs.

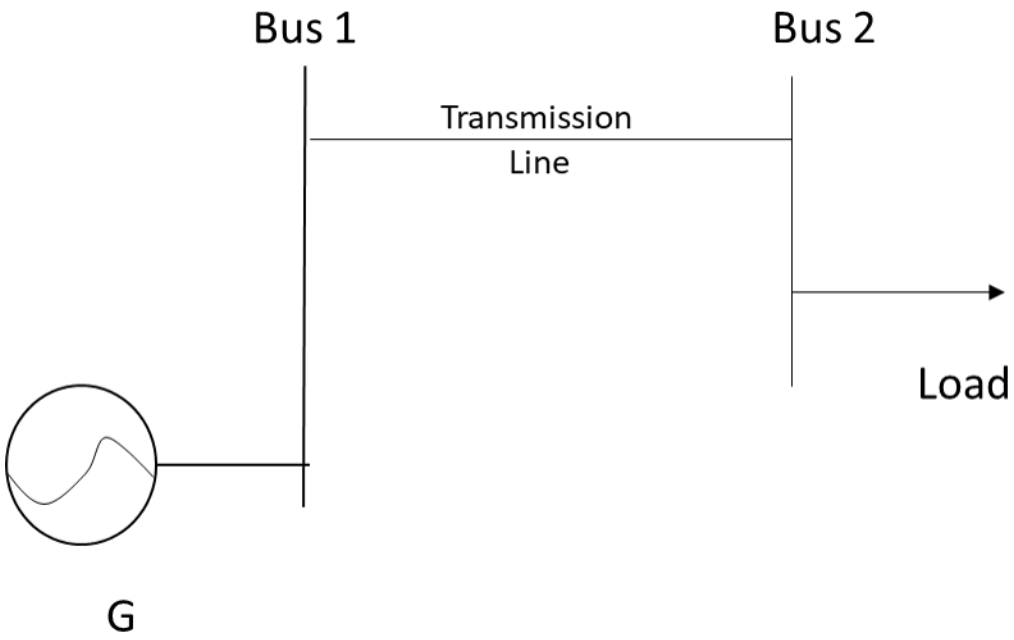

Figure 1.1: A 2-bus Power System

1.2 Literature Review of Bus Protection

There are different bus protection techniques that have been proposed in literature and used in practice. The following subsection explains bus protection techniques widely used.

1.2.1 Differential Protection

In differential protection as explained in [3-9], magnitudes of terminal currents are used to detect faults. Differential protection is based on Kirchhoff's current law. The sum of all the measured currents entering and leaving a bus must be zero unless there is a fault internal within the protection zone (bus fault). When there is no fault or if the fault is external from the protection zone (line fault), then the sum of all currents at the bus is zero or sum of all currents entering the zone is identical to the sum of all currents going out of the zone. During a bus fault, the bus provides the path for the flow of fault current that is not included in the calculation resulting in non-zero current summation. Differential protection is sensitive to CT saturation and CT mismatch and additional algorithms may need to detect the CT saturation and address its adverse effect [2]. Differential protection may mis-operate during close-in external faults because of CT saturation [8]. CT saturation during close-in external faults creates a high operating (differential) current making the sum of currents entering the zone not equal to the sum of the currents exiting the protection zone, causing undesired operation of the relay. The main reason for these undesired trips is that the differential principle works based on current magnitude rather than directionality for tripping decisions. Differential protection also needs directionality to maintain the integrity of discriminating faults in the protection zone from those outside the protection zone during close-in external faults as explained in [8]. A technique called Partial Operating Current (POC) explained in [5, 6] addresses the issues with differential protection including sensitivity to CT saturation and mis-operation during close-in external faults. The POC technique explained in [5, 6] calculate Partial Operating Current (POC) based on terminal currents that is used to discriminate the

internal fault and external fault for a current differential protection.

1.2.2 Directional Comparison Protection

In directional comparison protection explained in [2, 10-21], the direction of current is used to find the direction of the fault to discriminate between bus faults and line faults. The direction of all terminal currents connected to a zone of protection is towards the zone for a bus fault. The direction of one or more current terminals connected to a zone of protection is away from the zone for a line fault or normal operation. When compared to differential protection that only needs current from all terminals, directional protection needs current as well as voltage signals to determine the direction of the current. Two widely used directional comparison bus protection are voltage polarized directional element method and superimposed directional element method. The methods are explained further in the following subsections.

1.2.2.1 Voltage Polarized Directional Element Method

One of the methods in directional comparison protection is voltage-polarised directional element where two signals are needed to detect the direction of a fault. The two signals needed are operating phasor and polarising signal as explained in [2, 10-12]. The polarising signal is a reference quantity whose phase angle does not change before and after a fault. We use phase voltage, a different combination of phase voltage and sequence component as a polarising signal. The angular phase difference between operating and polarising signals determines the directionality for each terminal. This method uses a reference phasor assuming it is not distorted. However, this reference signal may be distorted which can result in wrong detection of the direction of the fault. Voltage-polarised directional element method needs

extensive filtering for correct measurements and hence a longer time for its operation during high impedance faults and high source impedance faults [2] where CVTs transient disrupts the voltage signal.

1.2.2.2 Superimposed Directional Element Method

The superimposed directional element operates based on the superposition theorem. Under the superposition theorem, each source and its effect are considered independently and the results are summed to determine a particular unknown quantity [2, 18]. In superimposed directional element method the post-fault value is a superposition of pre-fault value and fault generated value. In this directional comparison bus protection, the direction of the fault is detected by calculating fault generated value (superimposed value) by subtracting post-fault voltage and current with pre-fault voltage and current. The superimposed directional element method can be implemented in both the phasor-domain [12-14] and time-domain [15-21]. Superimposed method in phasor domain calculates the superimposed impedance by dividing subtracted post-fault phasor currents and voltages from pre-fault ones. A superimposed impedance lies in the first quadrant of the impedance plane when a fault is in the protection zone of the busbar. An impedance lies in the third quadrant when a fault is outside the protection zone of the bus [2,12]. The time-domain superimposed method finds the direction of the bus fault by getting superimposed value by subtracting the post-fault values of instantaneous currents and voltages from their pre-fault values as discussed in [2, 21]. The polarity of a superimposed value of instantaneous current and voltage is used to determine the direction of fault. The product of superimposed current and voltage is negative for a line fault and positive for a bus fault. The further development of the time-domain superimposed method

is to calculate the product of superimposed current and voltage which is a transient power and integrate this transient power over a certain period of time after fault inception to derive transient energy representing the fault [2, 18, 19, 20]. The time-domain superimposed method has been an effective method for ultra-high-speed fault detection in directional protection [2].

Based on the literature review [2, 4], CT saturation and CT ratio mismatch do not affect the performance of directional protection methods because directional protection methods only depend on voltage and current direction and not their magnitude. However, directional protection can be more expensive to implement because of the need of CVTs, which are not needed in differential protection. CVTs in directional protection are susceptible to transients during faults and could affect the accuracy of fault detection.

1.3 Scope and contribution of thesis

Considering the advantages and disadvantages of differential and direction protection methods, the goal of the thesis is to combine the robustness of directional protection against CT saturation and CT ratio mismatch while reducing the cost of implementation by excluding CVTs, which also helps to remove the transients of CVTs during faults. All directional comparison methods discussed above in directional comparison protection section need to have voltage signals along with the current signals to detect the direction of faults. Because of the CVTs, voltage polarized directional element method delays when detecting a high impedance fault. This thesis presents a new technique in directional comparison bus protection that removes the need of CVTs by incorporating partial operating current (POC) characteristics [5,6] used in differential protection. The superimposed component calculations used in time-

domain superimposed directional element method explained in [15-21] incorporate the POC characteristics are modified that detect the direction of fault without the use of CVTs. The proposed method is tested on a 4-bus test system and a practical power system model like IEEE 14-bus system to measure speed and accuracy of the method in detecting faults including the cases under severe CT saturation and high impedance faults. IEEE 14-bus test system helps to test the performance of proposed method in a real test system. To complete the thesis, the author reviewed POC method and time-domain superimposed directional element method which are explained in Chapter 2. In Chapter 3,the author explored the approaches to incorporate POC and to remove voltage signals from directional protection methods. The mathematical development of a new technique for directional comparison bus protection is also outlined in Chapter 3. In Chapter 4, test systems used to test the new technique are explained, including a 4-bus test system based on [5, 6, 15] and IEEE 14-bus system based on [22, 23]. Both test systems are modeled in Electro-Magnetic Transient Program (EMTP) while the proposed method algorithm is modeled in MATLAB. The test systems are subjected to various fault cases including severe CT saturation and high impedance faults.

The scope of the thesis can be highlighted as follows:

- Review POC and directional methods
- Formulate a new technique to determine the direction of fault that only need current signal.
- Implement the technique to discriminate bus fault and line fault in MATLAB.
- Build a 4-bus test system in EMTP and simulate test cases including severe CT saturation and high impedance fault.

- Build a practical real power system model IEEE 14-bus test system and simulate to test technique with real power system model for many test cases including severe CT saturation and high impedance fault.

- Compare the results of the proposed technique with POC technique [5,6] to compare the speed and accuracy to detect fault including severe CT saturation and high impedance faults.

Chapter 2

Mathematical Development

The review on development of superimposed component calculations based on superimposed directional element method [12-21] is included in this chapter. The author also summarizes the development of POC quantity based on POC characteristics [5, 6] which are used to discriminate the internal and external faults for differential protection. The author then explores the mechanism to exploit the advantages of the two methods – superimposed component method and POC method – for creating a new technique that accurately determines the direction of fault, yet removes the need of voltage signals in fault detection.

2.1 Superimposed Component Calculation

The superimposed component calculation is based on the superimposed directional element method. The superimposed directional element is a method for directional comparison bus protection. The directional comparison bus protection determines the direction of the current to discriminate the bus fault and line fault. The basic principle behind the direction protection is explained in Fig 2.1. Fig 2.1 shows a bus with three terminals connected to the bus. Fig 2.1 shows three operating conditions of the bus: normal condition, line fault, and bus fault. In Fig 2.1a the direction of I_1 and I_2 are towards the bus and direction of I_3 is outward from

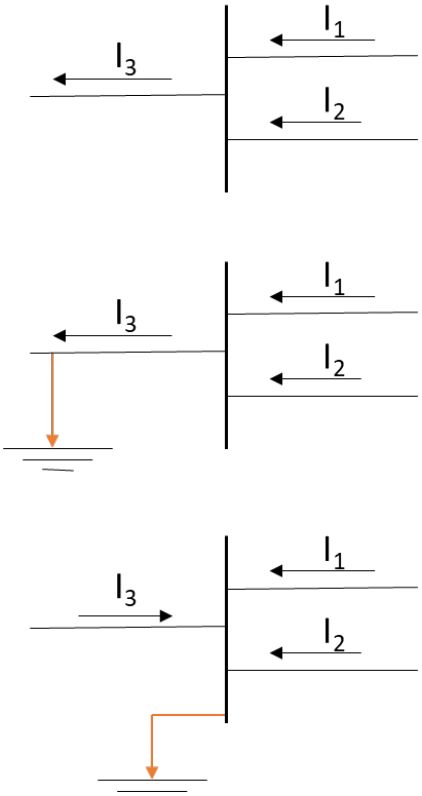

Figure 2.1: Basic Directional Principal a. Normal Condition b. Line Fault c. Bus Fault

the bus showing normal condition. Similarly during a line fault condition, the direction of faulted terminal current would be outside from the bus as shown in Fig 2.1b. But as shown in Fig 2.1c, for a bus fault the direction of currents of all terminals connected to the bus are towards the bus. This characteristic during a bus fault is used to discriminate bus fault from normal and line fault in directional comparison bus protection.

The superimposed directional element method determines the direction of all terminal currents to find direction of fault based on superposition theorem. The superposition theorem states that each source and its effect are considered independently and the results are summed to find the unknown quantity. The superimposed components for the post-faulted state can

be considered as a superposition of the pre-fault and fault generated quantities [2, 18].

$$Superimposed \quad Value(\Delta) = Postfault \quad component \quad - \quad Prefault \quad component \quad (2.1)$$

As shown in equation 2.1, the fault generated quantity superimposed value (Δ) would be subtracting post-fault component with the pre-fault component. The superimposed directional element method calculates the superimposed value of current (Δi) and voltage (Δv) shown in equation 2.2 and 2.3 respectively, and multiplication and division of the superimposed current and voltage are used to find the direction of fault.

For n-number of terminals connected to a zone of protection as shown in Fig 2.2, the directional superimposed method discussed in [2, 18-20] calculates superimposed current and voltage for each terminal k by subtracting an instantaneous sample of terminal current and voltage from its previous sample that was measured one time period before. The calculations are shown in equations 2.2 and 2.3.

$$\Delta i_{\phi k} = \sum_{j=g}^{g+N} i_{\phi k}(j) - i_{\phi k}(j-N) \quad \text{for} \quad k = 1, 2..n \tag{2.2}$$

$$\Delta v_{\phi k} = \sum_{j=g}^{g+N} v_{\phi k}(j) - v_{\phi k}(j-N) \quad \text{for} \quad k = 1, 2..n \tag{2.3}$$

In Equations 2.2 & 2.3, g represents the sample of the post-fault value, N the number of samples per cycle for each phase, and n number of terminals. $i_{\phi k}(j)$ is the current value of present sample of each phase and $i_{\phi k}(j-N)$ is the sample from one time period before. $v_{\phi k}(j)$ is the voltage value of present sample of each phase and $v_{\phi k}(j-N)$ is the sample from

one time period before.

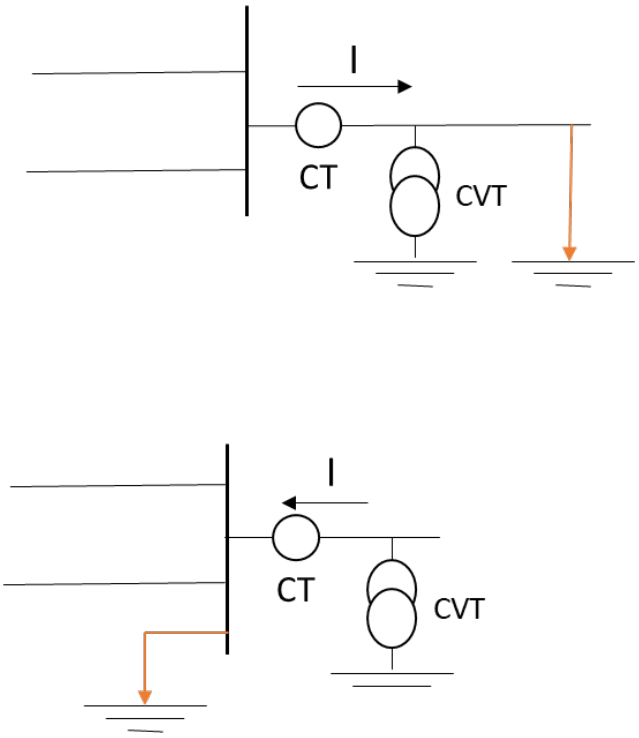

Figure 2.2: Superimposed Directional Element a. Line Fault b. Bus Fault

The superimposed directional element can be implemented in phasor-domain and time-domain. For phasor-domain it calculates the phasor value of current and voltage of each terminal measured from CTs and CVTs connected to each terminal and finds the superimposed values of current (ΔI) and voltage (ΔV). The superimposed values of current(ΔI) and voltage(ΔV) are used to calculate the (ΔV) /(ΔI) value to determine the direction of fault. For a line fault as shown in Fig 2.2a the value of (ΔV) /(ΔI) gives a negative impedance value showing current going outward from the bus. For a bus fault condition as shown in Fig 2.2b the value of calculated (ΔV) /(ΔI) will be positive. The value (ΔV) /(ΔI) for each terminal connected to a zone of the protection is calculated and if the (ΔV) /(ΔI) value is positive for every terminal then it is a bus fault otherwise a line fault.

The similar concept can be inferred in the time-domain method but the instantaneous

values of current and voltage are used to determine the direction of terminal currents. The instantaneous values of the current and voltage of each terminal are measured by the respective CTs and CVTs and superimposed current and voltage are calculated based on equations 2.2 and 2.3. The instantaneous current and voltage are multiplied together, ($\Delta v \times \Delta i$), to determine the direction of the corresponding terminal current. For a line fault shown in Fig 2.2a the $\Delta i \times \Delta v$ gives a negative value while for a bus fault shown in Fig 2.2b $\Delta i \times \Delta v$ gives a positive value. The $\Delta i \times \Delta v$ for each terminal connected to a zone of the protection is calculated and if the $\Delta i \times \Delta v$ value is positive for every terminal then it is a bus fault otherwise a line fault.

The superimposed directional element need to have both current and voltage signals to determine the direction of the fault. The next section reviews POC characteristics method that calculates the partial operating currents to discriminate the internal and external faults for current differential protection.

2.2 Partial Operating Current (POC) Characteristics

The partial operating current (POC) based on POC characteristics [5, 6] is used in discriminating internal and external faults for differential protection. Any method under differential protection is based on Kirchhoff's current law which states that the sum of all currents measured around the zone of protection for normal and external faults sum up to zero. In Fig 2.3 we can see five terminal currents coming to the zone and one terminal going out of the zone. According to Kirchhoff's law, the sum of the currents must be equal to zero for

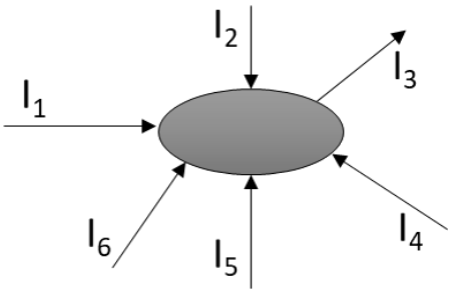

Figure 2.3: Basic Differential Principal

normal operation as shown in equation 2.4.

$$I_1 + I_2 + I_3 + I_4 + I_5 + I_6 = 0 \tag{2.4}$$

$$I_1 + I_2 + I_3 + I_4 + I_5 + I_6 = I_{diff} \tag{2.5}$$

Similarly, currents summing to non-zero would indicate a fault in the zone. When sum of all the currents around the protection zone is equal to some differential current I_{diff} shown in equation 2.5 then it would represent internal bus fault. The I_{diff} value would be zero ($I_{diff} = 0$) for external fault or normal condition. The POC characteristics [5, 6] based on Kirchhoff's current principle provide a technique that calculates POC (partial operating current) that is used to discriminate internal and external faults successfully for differential protection.

In Fig 2.4, n terminals are connected to the zone of protection. The POC equated by (2.6) is a quantity which is a successive addition of a phasor terminal current [5, 6].

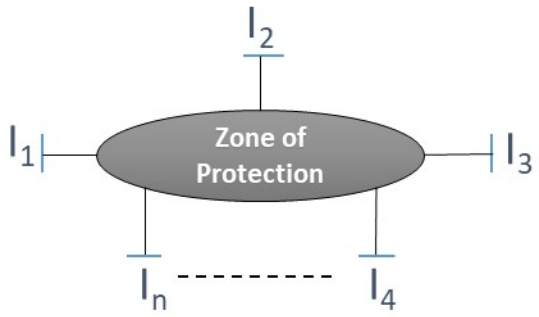

Figure 2.4: n-terminal protection zone

$$I_{\phi op(k)} = \sum_{j=1}^{j=k} I_{\phi(j)} + I_{\phi(k+1)} \quad \text{for} \quad k = 1, 2..n-1 \tag{2.6}$$

As explained in [5], $I_{\phi op(k)}$ in (2.6) is the k^{th} POC and an n-terminal zone has *n-1* POCs. From Equation (2.6), the relationship between consecutive POCs is shown in (2.7).

$$I_{\phi op(k)} = I_{\phi op(k-1)} + I_{\phi(k+1)} \quad \text{for} \quad k = 1, 2, ...n-1 \tag{2.7}$$

$I_{\phi op(k)}$ is the resultant current that has two inputs currents $I_{\phi op(k-1)}$ & $I_{\phi op(k+1)}$.

Operation of a power system is based on three operating conditions: normal condition, bus faults and line faults. Bus faults are faults within the zone of protection and line faults are faults outside the zone of protection. The desired bus protection is to discriminate between bus faults and line faults so that the zone trips for bus faults only. The POC characteristics representing the three operating conditions of an n-terminal protection zone explained in [5] are shown in Equations (2.8) to (2.10). Equation (2.8) is for normal condition. Equation (2.9) represents line fault condition where r represents a faulted terminal. Equation (2.10) represents bus fault condition where k = 1, 2, ..., (n-1).

$$|I_{\phi op(n-1)}| < max(|I_{\phi op(n-2)}|, |I_{\phi n}|) \tag{2.8}$$

$$|I_{\phi op(r)}| < max(|I_{\phi op(r-1)}|, |I_{\phi (r+1)}|) \tag{2.9}$$

$$|I_{\phi op(k)}| > max(|I_{\phi op(k-1)}|, |I_{\phi (k+1)}|) \tag{2.10}$$

In normal condition, for an n-terminal directional protection zone having each terminal current greater than zero, the sum of all terminal currents must be equal to zero according to Kirchhoff's current law. Based on Kirchhoff's current law and Equation (2.7), at least one resultant POC magnitude has magnitude smaller than the larger one of its two input currents [5], as shown in Equation (2.8).

For line fault condition, the current flows outward from zone of protection [23] to the faulted terminal so that direction of current is different at faulted terminal compared to other terminals that are not faulted. In general, the sum of all phasor currents is zero for a line fault and POC behaves the same way as in normal operating condition. But, if the CT is saturated then summation of all the terminal currents may not be zero. Equation (2.9) as developed in [5] explains that at least one of the resultant POC is smaller than the larger one of its two input currents for any direction protection zone during a line fault irrespective of CT saturation.

The bus fault is the internal fault to zone of protection. All terminal currents flow towards the zone and are in same phase as described in [25]. During CT saturation, there can be a large phase difference between saturated terminal and unsaturated terminal while the secondary current magnitude decreases and its angle advances [26]. However, when angle

distortion approaches to 90 degrees, the magnitude approaches to zero [27] making maximum phase difference between any two terminals less than 90 degrees even if CT saturates. This means that all terminals are in the same direction irrespective of CT saturation. We can say that the resultant $I_{\phi op(k)}$ from (2.2), is in the same direction with its two input currents $I_{\phi op(k-1)}$ and $I_{\phi(k+1)}$ during a bus fault for k = 1, 2, ..., (n-1) because the possible maximum angle between any two POC's input currents is $< 90°$. Equation (2.10) derived from (2.7) in [5] can therefore be used to detect bus faults. Equation (2.10) defines that each resultant POC is greater than the larger one of its two input currents when there is a bus fault.

The superimposed directional element method provides simple, fast calculations to detect a bus fault hence the method is widely used in directional protection. The method requires both voltage and current signals in its calculations. The POC method does not require voltage signals and the method has simple computation for all conditions in discriminating bus faults from other types of faults. The author will demonstrate in Chapter 3 a technique developed to incorporate the POC method into the superimposed directional element method in order to remove the voltage signals required in the superimposed method for directional protection.

Chapter 3

Proposed Method

After the review of POC characteristics and superimposed current, the author proposes a new technique to determine the direction of a fault that only needs current signals. The new technique essentially modifies the POC method by applying superimposed current to POC currents, which will be referred to as superimposed POC (SPOC). This modification allows the new technique to detect a fault based on a directional comparison method without the use of CVTs. Fig 3.1 presents a proposed block diagram of SPOC which only has current signal inputs to detect a fault. As seen in Fig 3.1 current terminals are an input to the superimposed block that gives out superimposed terminal currents ΔI_n. These output superimposed terminal currents are then inputted to SPOC (superimposed partial operating current characteristics) block that discriminates in-zone faults from out-of-zone faults based on

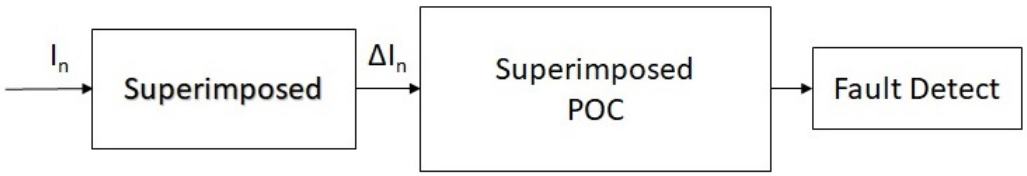

Figure 3.1: Proposed Block Diagram of Superimposed POC (SPOC)

POC characteristics represented by Equations (2.8) to (2.10). The overview of a mathematical development of SPOC using the superimposed current and POC characteristics is explained in this chapter. The formulation of SPOC resulting in equation (3.3) that is used to discriminate bus faults from line faults and normal condition for any fault cases without the use of CVTs [15] is explained in section 3.1 of this chapter. The flowchart of a proposed algorithm and an approach to implementing the SPOC technique are explained in section 3.2 of this chapter.

3.1 Superimposed Partial Operating Current (SPOC)

Superimposed current $\Delta i_{\phi k}$ from (2.2) is used in converting POCs of (2.6) and (2.7) into superimposed POCs. Superimposed POCs shown in (3.1) are modified POCs from (2.6) by using the superimposed current of (2.2) based on superimposed directional element method explained in section 2.2.

$$\Delta I_{\phi op(k)} = \sum_{j=1}^{j=k} \Delta I_{\phi(j)} + \Delta I_{\phi(k+1)} \quad \text{for} \quad k = 1, 2..n-1 \tag{3.1}$$

In Equation (3.1) the $\Delta I_{\phi op(k)}$ is the k^{th} superimposed POC. Similar to POCs, the relationship between consecutive superimposed POCs can be expressed by Equation (3.2).

$$\Delta I_{\phi op(k)} = \Delta I_{\phi op(k-1)} + \Delta I_{\phi(k+1)} \quad \text{for} \quad k = 1, 2, ...n-1 \tag{3.2}$$

In Equation (3.2), the k^{th} superimposed POC $\Delta I_{\phi op(k)}$ is the phasor sum of the previous superimposed POC $\Delta I_{\phi op(k-1)}$ and the next superimposed terminal current $\Delta I_{\phi k+1}$.

Using the same approach of converting POCs to superimposed POCs shown in (2.1,

2.2, 2.6, 3.1, 3.2) each POC $I_{\phi op(k)}$ in bus fault condition of (2.7) can be converted to superimposed POC $\Delta I_{\phi op(k)}$ and terminal current $I_{\phi k}$ to superimposed terminal current $\Delta I_{\phi k}$. POC characteristic for bus fault condition of Equation (2.7) modified with superimposed POC becomes Equation (3.3) shown below.

$$|\Delta I_{\phi op(k)}| > max(|\Delta I_{\phi op(k-1)}|, |\Delta I_{\phi(k+1)}|) \tag{3.3}$$

In (3.3), k = 1, 2,.., (n-1) and each resultant superimposed POC $|\Delta I_{\phi op(k)}|$ is greater than the larger one of its two input superimposed currents $|\Delta I_{\phi op(k-1)}|$ and $|\Delta I_{\phi(k+1)}|$ for any n-terminals connected to zone of protection for a bus fault. Equation (3.3) is used to discriminate a bus fault from a line fault and normal condition [15].

During a high impedance bus fault, a small current flows through passive elements. The POC algorithm [5] would need to exclude this current from its algorithm because the current flowing outwards is considered a line fault. Using superimposed POC does not need to exclude such current. The pre-fault phasor of a terminal current flowing outwards to a passive element is larger in magnitude than the post-fault value. Hence the direction of superimposed current of the terminal is always the opposite of the pre-fault current, which is towards the bus, not considered a line fault. Therefore, the proposed superimposed POC does not need to exclude any current.

The formulated superimposed POC (SPOC) Equation (3.3) helps to discriminate bus faults from line faults and normal condition for any fault cases including CT saturation and high impedance faults. This equation is used in the proposed algorithm to detect a bus fault without the use of CVTs.

3.2 Approach

Fig 3.2 shows the flowchart of the implementation of mathematical development of proposed SPOC algorithm. The proposed method in Fig. 3.2 starts with taking in instantaneous terminal currents and finds the superimposed terminal currents $\Delta i_{\phi k}$ using Equation (2.6) by subtracting the post-fault value from the pre-fault value. The superimposed terminal currents $\Delta i_{\phi k}$ are then converted to phasor quantity using Fast Fourier Transform (FFT). POC calculator in Fig. 1 uses Equation (3.3) to calculate the superimposed POCs $\Delta I_{\phi op(k)}$ using the phasor of superimposed terminal currents $\Delta I_{\phi k}$. The superimposed POC at k^{th} terminal is phasor sum of the previous superimposed POC and next superimposed terminal current with initial condition of $\Delta I_{\phi op(0)}$=$\Delta I_{\phi(1)}$. The output of POC Calculator, $\Delta I_{\phi op(k)}$, is (*n-1*) superimposed POCs that are compared according to Equation (3.3) to detect a bus fault. In Equation (3.3), superimposed POC at k^{th} terminal must be higher in magnitude than previous superimposed operating current and next superimposed terminal current that are two of the inputs. If Equation (3.3) is satisfied for all SPOCS, the method results in a trip for a bus fault. If at least one of the SPOCs does not satisfy Equation (3.3), the method will not trip the protected bus. The result of the method can then be displayed or recorded. The cycle from Start to Display repeats as the algorithm continues to monitor the protected bus.

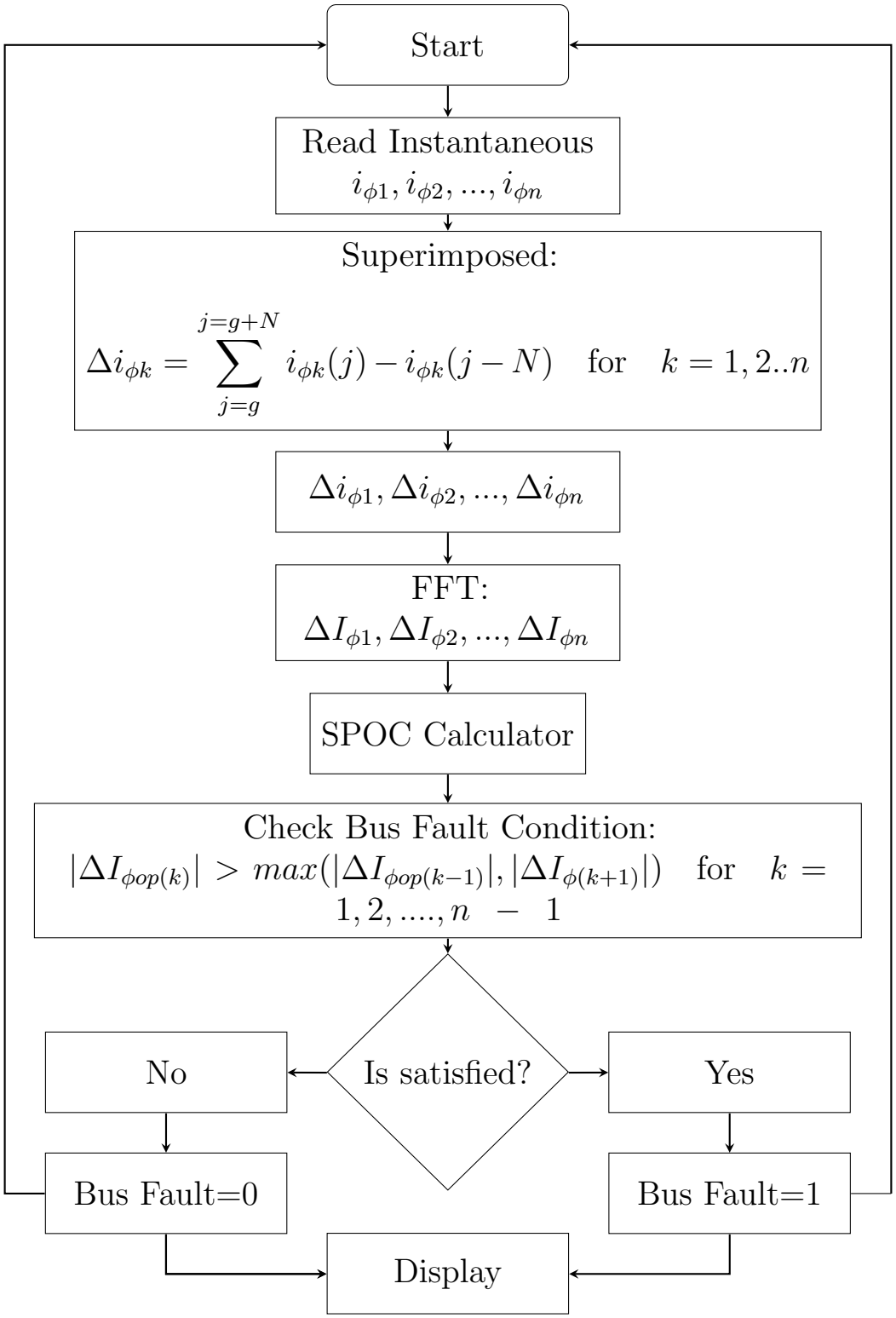

Figure 3.2: Flow chart of Proposed Algorithm

The approach to implementing the proposed technique is explained in Fig 3.3. A test system is modeled in Electro-Magnetic Transient Program (EMTP). The test system is simulated under various fault impedances including severe CT saturation and high impedance faults. Instantaneous currents from the simulations in EMTP are captured as a .txt file. The text file is then used as an input to the algorithm model of Fig 3.2. The algorithm is implemented in MATLAB and the results of the algorithm are recorded.

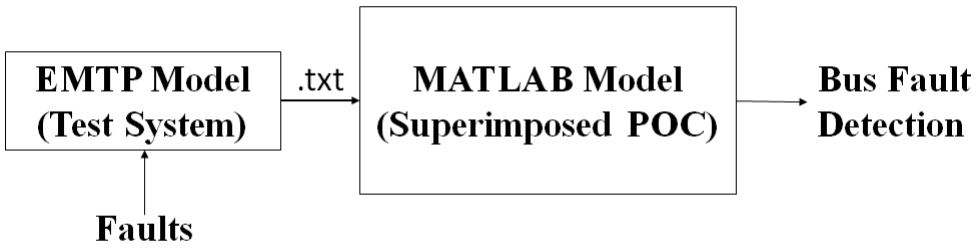

Figure 3.3: Approach of the Proposed Method

The approach in Fig 3.3 will be used to test the proposed SPOC method by applying the approach to a 4-bus test system and IEEE 14-bus test system. The details of each of two test systems are explained in chapter 4. The results of the simulations will be presented and discussed in chapter 5.

Chapter 4

Simulation Tools and Test Systems

This chapter provides an overview of simulation tools and test systems used in implementing the proposed approach explained in Fig 3.3. The algorithm of SPOC method explained in Fig 3.2 is implemented in MATLAB. EMTP is used to build, simulate and capture the test system. The captured instantaneous currents in EMTP are input to MATLAB for testing the proposed SPOC algorithm.

4.1 Simulation Tools

4.1.1 MATLAB

The name MATLAB stands for Matrix Laboratory. MATLAB is a technical computing environment for high-performance numeric computations and visualizations. It is a technical computing language developed by Mathworks Inc. MATLAB integrates numerical analysis, matrix computation, signal processing, and graphics into an easy-to-use environment.

The algorithm presented in Fig 3.2, and Equation (3.3) used to discriminate the bus faults from line faults without the need of CVTs, are implemented in MATLAB. MATLAB code is included in Appendices A.3 and A.4 for 4-bus test system and 14-bus test system, respectively. The instantaneous currents that are input to the MATLAB are generated by

EMTP as a .txt file which is explained in the next subsection.

4.1.2 EMTP

EMTP is an acronym for Electromagnetic Transients Program. EMTP is a software tool that is used by power systems engineers to analyze electromagnetic transients. It is suited for a wide variety of power system studies whether they relate to project, design, and engineering, or to solve problems and unexplained failures. It is capable of efficiently and quickly performing a simulation of very large power systems. Its numerical robustness and the stability of the simulation engine contribute to make EMTP-RV the reference for power systems transients. EMTP's has a standard library that provides a comprehensive and well-documented list of components and function blocks that allow the user to conduct complete and complex power system studies.

EMTP in this thesis is used to model two test systems, 4-bus [5, 6] and IEEE 14-bus [22], which are subjected to various fault cases including severe CT saturation and high impedance fault. The instantaneous value of the currents are captured in .txt file and input to MATLAB where the proposed algorithm of Fig 3.2 is implemented.

4.2 Test System

The two test systems are modeled in EMTP that are subjected to severe CT saturation and high impedance fault. The first test system is a simple 4-bus test system that is designed based on [5, 6, 15] and the next is IEEE 14-bus test system based on [22, 23].

4.2.1 4-bus Test System

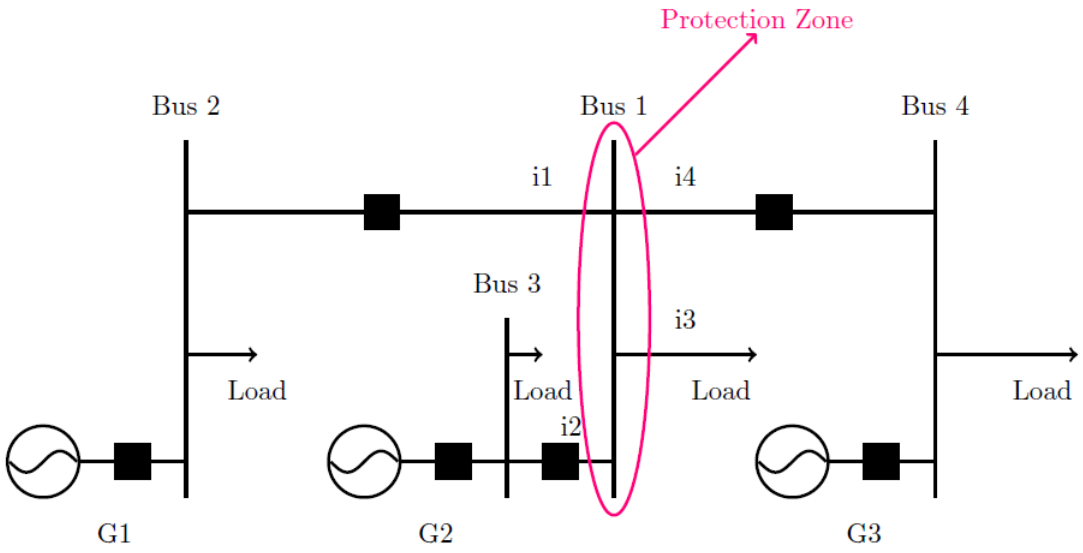

Figure 4.1: Four Bus Test System

The 4-bus test system model shown in Fig 4.1 is created based on the model presented in papers [5, 6, 15]. Fig. 4.1 shows four bus 230 kV test system with Bus 1 as a zone of protection with four terminals connected to the zone. Three of the four terminals at Bus 1 have an active source at their far end and the fourth terminal is connected directly to a passive element (load). The test system model shown in Fig 4.1 is built in EMTP as shown in Fig 4.6.A constant distributed parameter model [28] is used for transmission lines. The CTs are modeled to include the effect of saturation [29]. The ratio of the CTs used in this test is 1000/5. The created test model of Fig 4.1 is validated by comparing system responses under normal operation and under a fault. The responses under normal operation from the papers [5, 6, 15] shown in Fig 4.3 are compared with the resposnes from the EMTP model built for this thesis as shown in Fig. 4.2. Similar comparison when the system is under a

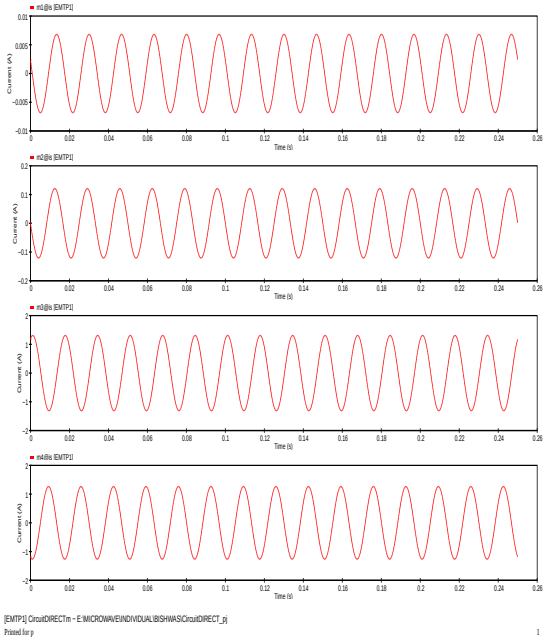

Figure 4.2: Steady State Terminal Currents of 4-bus Test System of Fig 4.1

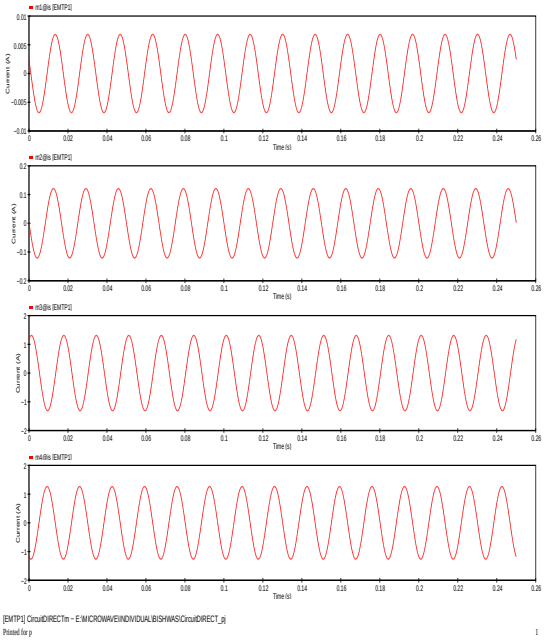

Figure 4.4: Steady State Terminal Currents of 4-bus Test System of [5, 6, 24]

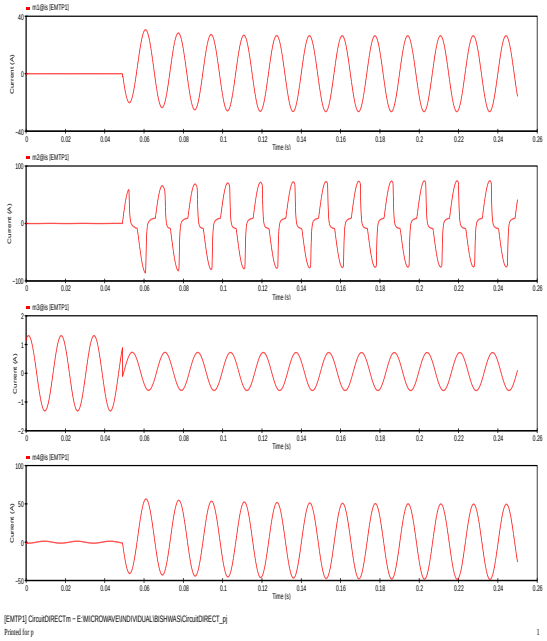

Figure 4.3: Dynamic State Terminal Currents of 4-bus Test System of Fig 4.1

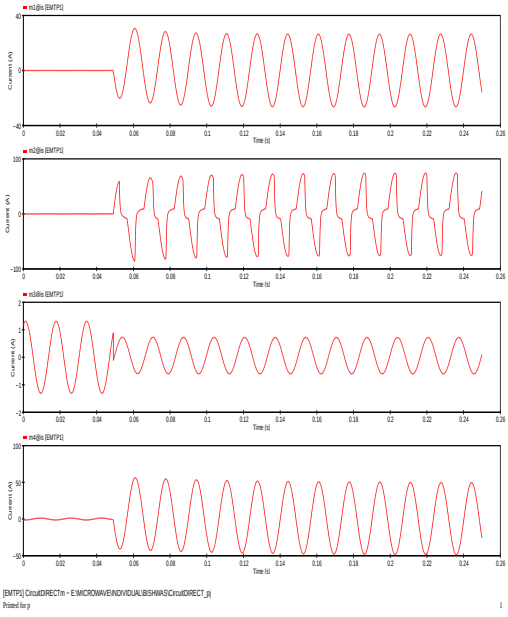

Figure 4.5: Dynamic State Terminal Currents of 4-bus Test System of [5, 6, 24]

fault is shown in Fig 4.4 & 4.5, where Fig 4.4 is generated by the author's EMTP model and Fig. 4.5 is from the references [5, 6, 15].

The test system is simulated in EMTP with a sampling rate of 200 samples per cycle. The measured A-phase instantaneous CT secondary currents at four terminals simulated in EMTP are i_1, i_2, i_3 and i_4, respectively. The four instantaneous currents are input to the

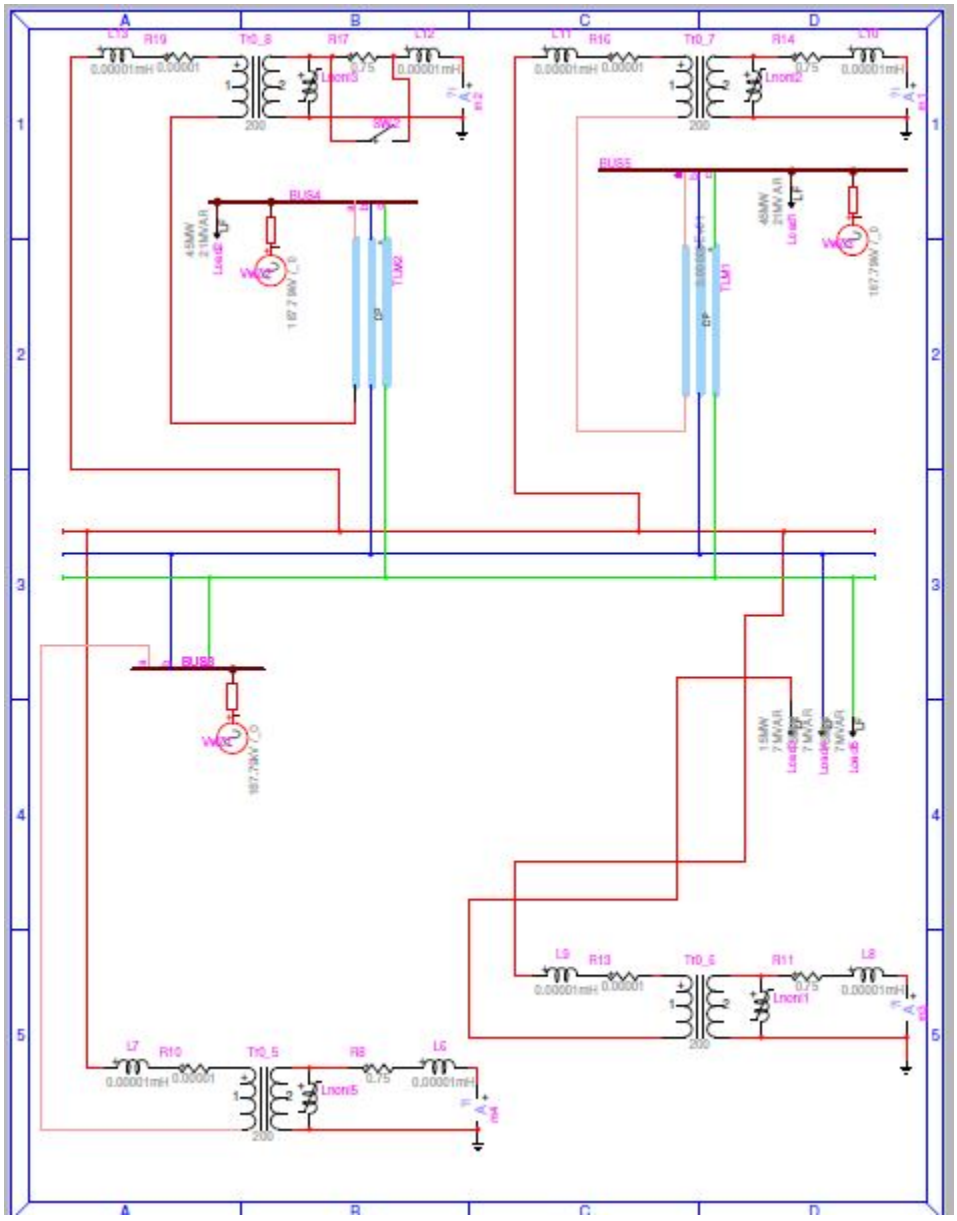

Figure 4.6: Four Bus Test System in EMTP

MATLAB to find superimposed currents, phasors and POC values. The algorithm of Fig. 3.2 is implemented in MATLAB to calculate superimposed terminal currents ($\Delta I_1, \Delta I_2, \Delta I_3, \Delta I_4$) and superimposed POCs ($\Delta I_{op1}, \Delta I_{op2}, \Delta I_{op3}$) and to detect bus faults based on equation (3.3) using the magnitude of the calculated superimposed POCs. If (3.3) is satisfied then the algorithm declares a bus fault at Bus 1, which is the zone of protection.

4.2.2 IEEE 14-bus Test System

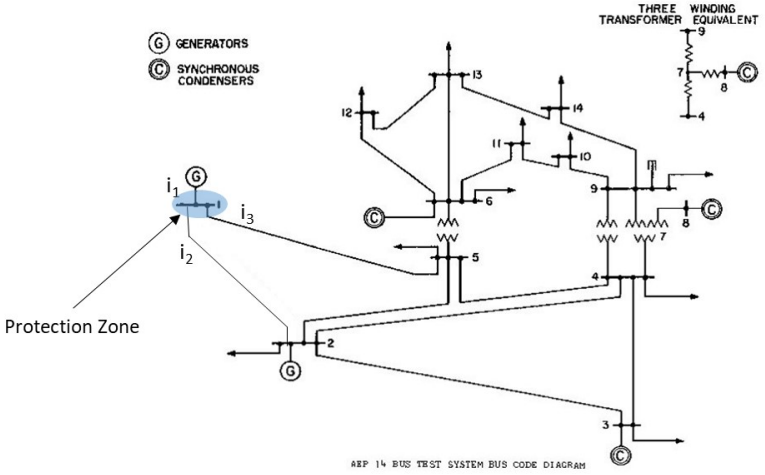

Figure 4.7: IEEE 14-bus Test System

IEEE 14-bus System is created based on the model presented in a masters thesis [22]. The IEEE 14-bus test system is an equivalent system of a portion of the American Electric Power System (in the Midwestern US) as of February 1962. It has 14 buses, 2 synchronous generators, 3 synchronous condensers, 1 shunt capacitor, 3 transformers (2 two-winding, 1 three-winding), 11 loads and 18 transmission lines (considering the two-winding equivalent of the three-winding transformer) [22, 23]. For simplicity, a two-winding equivalent of the three winding transformer which is originally in the system is used. The double line between bus-1 and bus-2 is converted to a single line. The system's base voltage is 138 kV with 100

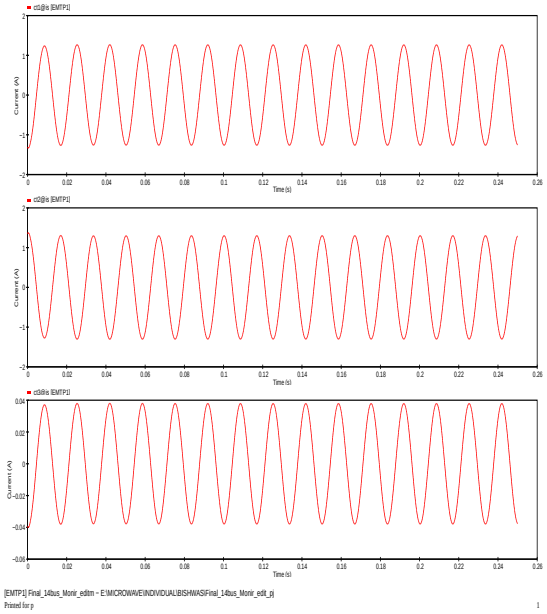

Figure 4.8: Steady State Terminal Currents of IEEE 14-bus Test System of Fig 4.7

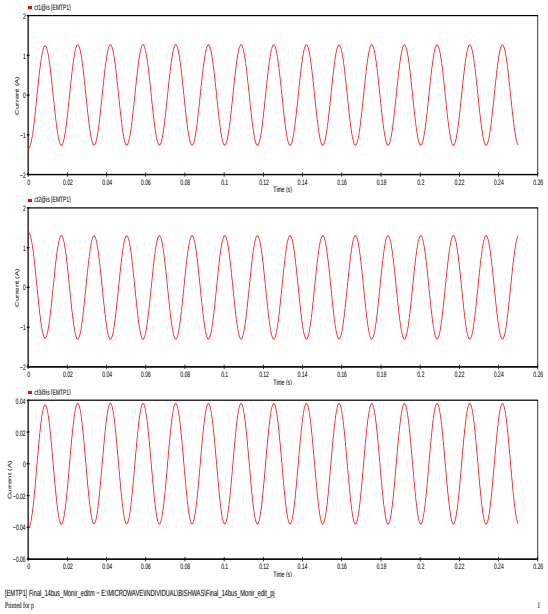

Figure 4.9: Steady State Terminal Currents of IEEE 14-bus Test System of [22, 23]

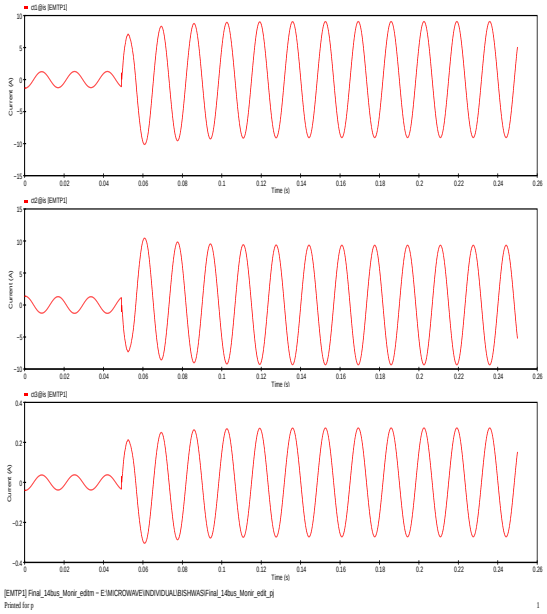

Figure 4.10: Dynamic State Terminal Currents of IEEE 14-bus Test System of Fig 4.7

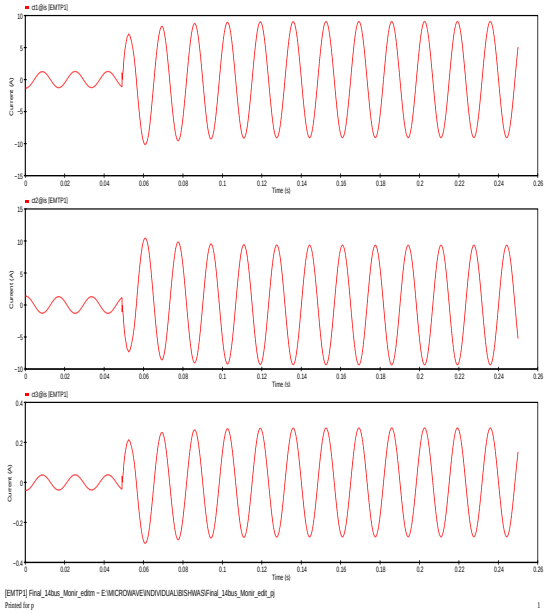

Figure 4.11: Dynamic State Terminal Currents of IEEE 14-bus Test System of [22, 23]

MVA power base. The total load of the system is 254 MW and 73.4 MVar [22, 23]. Bus-1 is considered slack/swing bus.

The test system shown in Fig 4.7 has bus-1 as a zone of protection with three terminals connected to the zone. The terminal from generator to bus-1 is i_1, terminal from bus-1 to bus-2 is i_2, and terminal from Bus-1 to bus-5 is i_3. Terminal i_1 has an active source connected to it and Terminal i_2 has an active source connected to its far end. The test system model shown in Fig 4.7 is built in EMTP as shown in Fig 4.12. Similar to the 4-bus system the CTs are modeled to include the effect of saturation [29]. The ratio of the CTs used in this test system is 1000/5. The simulated responses of Fig 4.7 from the author's EMTP model are captured in Fig. 4.8 under normal condition and in Fig. 4.10 under a fault. The responses in Fig. 4.8 and Fig. 4.10 are validated by comparing to the responses from Masters thesis paper [22, 23] shown in Fig 4.9 for normal condition and Fig 4.11 for a faulted condition.

The test system is simulated in EMTP with sampling rate of 200 samples per cycle. The measured A-phase instantaneous CT secondary currents at three terminals simulated in EMTP are i_1, i_2, and i_3 respectively. The three instantaneous currents are input to the MATLAB to find superimposed currents, phasors and POC values. The algorithm of Fig. 3.2 is implemented in MATLAB to calculate superimposed terminal currents ($\Delta I_1, \Delta I_2, \Delta I_3$) and superimposed POCs ($\Delta I_{op1}, \Delta I_{op2}$) and to detect bus faults based on equation (3.3) using the magnitude of the calculated superimposed POCs. If (3.3) is satisfied than the algorithm declares a bus fault at Bus 1, which is the zone of protection.

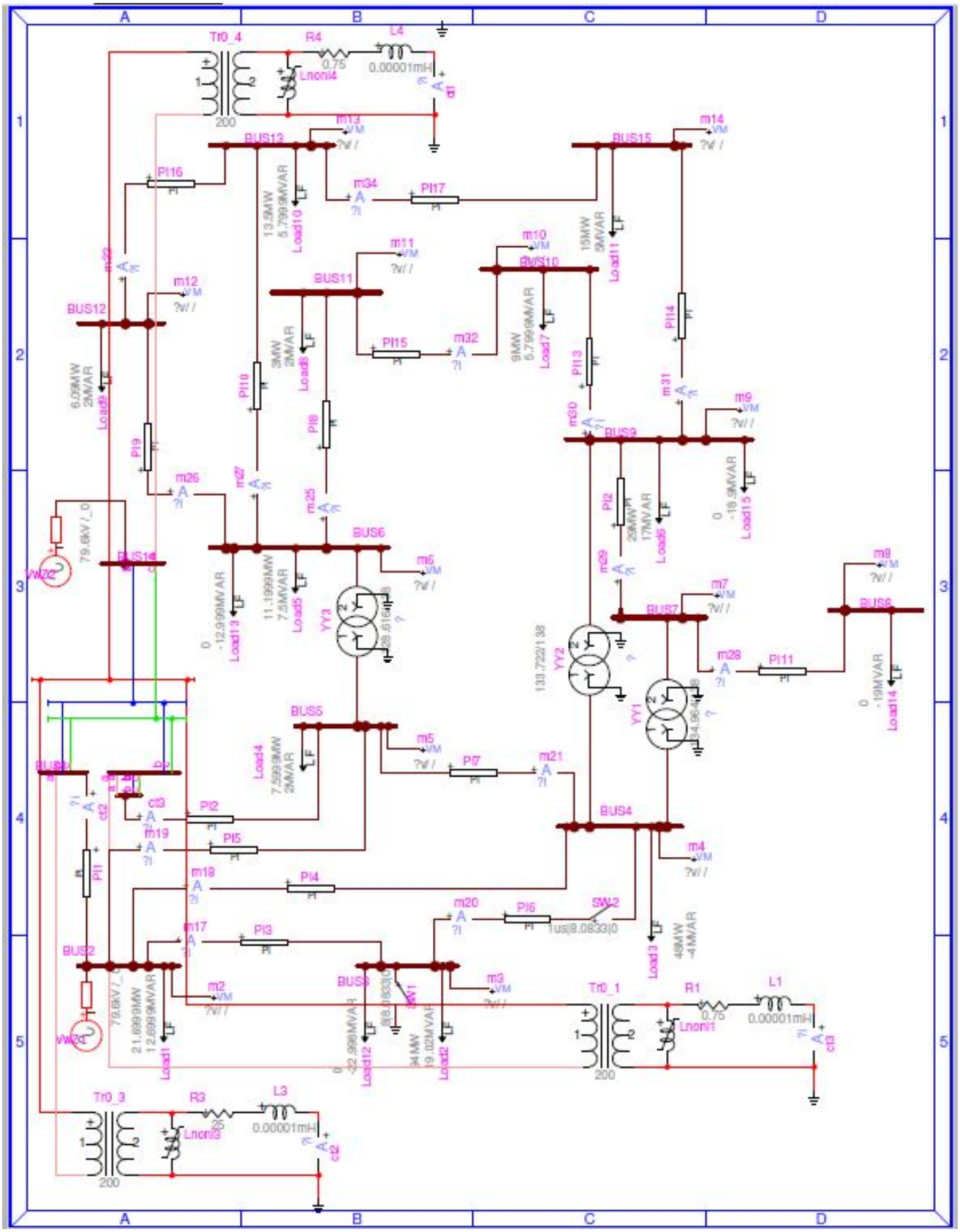

Figure 4.12: IEEE 14-bus Test System in EMTP

Chapter 5

Simulations and Results

This chapter provides an overview of test cases and corresponding results of the proposed algorithm. The chapter is divided into two sections. Section 5.1 presents results of the algorithm from the 4-bus system simulations and Section 5.2 shows results from IEEE 14-bus system simulations. The test cases include single phase to ground, phase-phase, and phase-phase to ground subjected to severe CT saturation and high impedance faults. The SPOC algorithm outputs either a bus fault or an external fault corresponding to each of the test cases. The chapter uses all cases to determine the performance of the proposed SPOC algorithm and discusses specific cases in detail. The results of the SPOC algorithm is then compared to the POC method of [5, 6]. The comparison is summarized in Table 5.6 and Table 5.12 for 4-bus and IEEE 14-bus systems, respectively. The accuracy and speed of both SPOC and POC are compared.

5.1 4 Bus Test System

5.1.1 Test Cases

Fault detection by the SPOC algorithm for various fault cases is listed in Table 5.1. Z_f represents the fault impedance. The different types of bus faults and line faults such as

phase to phase, phase-phase to ground, and phase to ground, with various fault impedances and locations, are tested and reported in Table 5.1. The fault is induced at 49 ms for every test case. The timing of fault detection for every bus fault is shown as Detection Delay in milliseconds in Table 5.1. NA represents the test cases that the algorithm does not detect bus faults because the faults are external from the viewpoint of the bus. The proposed method is fast with the fault detection within 0.15 ms after fault inception. The method accurately discriminates bus faults and line faults for all test cases shown in Table 5.1 including various severe CT saturation and high impedance faults. For example, a bus fault of high impedance Z_f= 200 Ω is detected successfully by the method within 0.15 ms time.

Table 5.1: Test Cases 4-bus Test system

Fault	Location	Z_f	Time(ms)		System Response
		(Ω)	Inception	Detection Delay	
AB	Terminal 2	0.1	49	NA	Line Fault
AB	Terminal 2	5	49	NA	Line Fault
AB	Terminal 2	10	49	NA	Line Fault
AG	Terminal 2	0.1	49	NA	Line Fault
AG	Terminal 2	5	49	NA	Line Fault
AG	Terminal 2	10	49	NA	Line Fault
ABG	Terminal 2	0.1	49	NA	Line Fault
ABG	Terminal 2	5	49	NA	Line Fault
ABG	Terminal 2	10	49	NA	Line Fault
AB	Bus 1	0.1	49	0.15	Bus Fault
AB	Bus 1	5	49	0.15	Bus Fault
AB	Bus 1	10	49	0.15	Bus Fault
ABG	Bus 1	0.1	49	0.15	Bus Fault
ABG	Bus 1	5	49	0.15	Bus Fault
ABG	Bus 1	10	49	0.15	Bus Fault
AG	Bus 1	0.1	49	0.15	Bus Fault
AG	Bus 1	5	49	0.15	Bus Fault
AG	Bus 1	50	49	0.15	Bus Fault
AG	Bus 1	100	49	0.15	Bus Fault
AG	Bus 1	200	49	0.15	Bus Fault

5.1.2 Discussion of Results

Four out of twenty cases are the key fault cases that are explained in detail with the waveforms captured from MATLAB simulations in the following subsection. Waveforms of all other test cases not discussed in this section are available for review in Appendix A.1.

5.1.2.1 Phase-Phase Line fault with CT Saturation

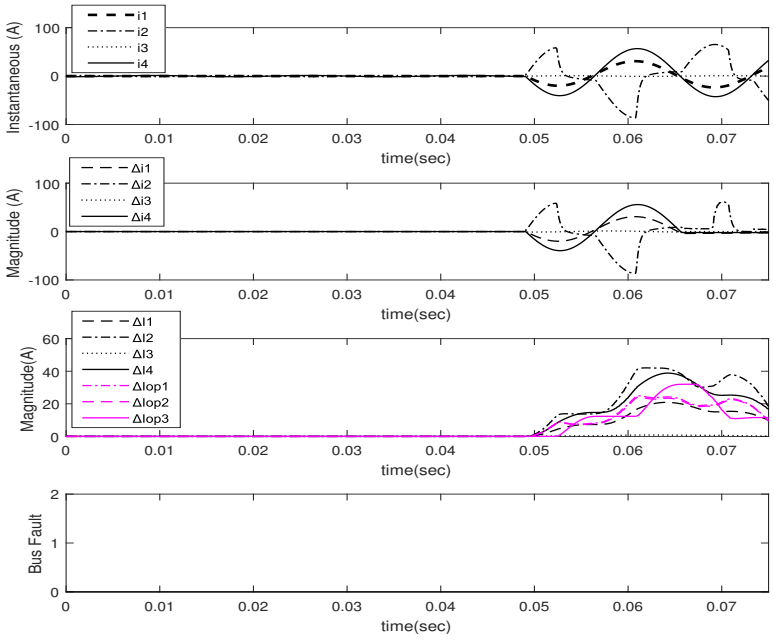

Figure 5.1: Phase-Phase Line Fault with CT saturation at 49ms a. Instantaneous Current, b. Superimposed Current, c. Superimposed Current Phasor Magnitude and Superimposed POC magnitude d. Fault Discriminator

Fig. 5.1 shows Phase-Phase line fault at terminal 2 which caused i_2 to get distorted because of CT saturation. Fig. 5.1a shows Phase-Phase line fault at terminal 2 which caused i_2 to get distorted because of CT saturation. The fault impedance was Z_f= 0.1 Ω. Fig. 5.1b shows superimposed instantaneous current $(\Delta i_1, \Delta i_2, \Delta i_3, \Delta i_4)$ values. The

magnitude of superimposed terminal currents ($\Delta I_1, \Delta I_2, \Delta I_3, \Delta I_4$) and superimposed POCs ($\Delta I_{op1}, \Delta I_{op2}, \Delta I_{op3}$) are shown in Fig. 5.1c. At time $t = 50ms$ in Fig. 5.1c, the values of $\Delta I_1, \Delta I_2, \Delta I_3, \Delta I_4, \Delta I_{op1}, \Delta I_{op2}, \Delta I_{op3}$ are shown in Table 5.2. In Fig. 5.1c, the magnitude of $\Delta I_{op1} < max(\Delta I_1, \Delta I_2)$, $\Delta I_{op2} < max(\Delta I_{op1}, \Delta I_3)$ and $\Delta I_{op3} < max(\Delta I_{op2}, \Delta I_4)$ for entire time period of the fault, thus not satisfying the bus fault condition of Equation (3.3). Therefore, the bus fault output of the algorithm shown in Fig. 5.1d is set to zero, representing a line fault which is external to the zone of protection.

Table 5.2: Phase-Phase Line Fault Superimposed Currents & SPOCs Values

At Time, t=50ms						
ΔI_1	ΔI_2	ΔI_3	ΔI_4	ΔI_{op1}	ΔI_{op2}	ΔI_{op3}
0.4462	1.3340	0.0974	0.7914	0.8877	0.7906	0.0008
$\angle 173.45°$	$\angle -6.07°$	$\angle 169.52°$	$\angle 174.57°$	$\angle -5.98°$	$\angle -5.43°$	$\angle 175.84°$

5.1.2.2 Phase-Phase to Ground Line Fault with CT Saturation

Fig. 5.2a shows Phase-Phase line fault at terminal 2 which caused i_2 to get distorted because of CT saturation. The fault impedance was Z_f= 0.1 Ω. Fig. 5.2b shows superimposed instantaneous current ($\Delta i_1, \Delta i_2, \Delta i_3, \Delta i_4$) values. The magnitude of superimposed terminal currents ($\Delta I_1, \Delta I_2, \Delta I_3, \Delta I_4$) and superimposed POCs ($\Delta I_{op1}, \Delta I_{op2}, \Delta I_{op3}$) are shown in Fig. 5.2c. At time $t = 50ms$ in Fig. 5.2c, the values of $\Delta I_1, \Delta I_2, \Delta I_3, \Delta I_4, \Delta I_{op1}, \Delta I_{op2}, \Delta I_{op3}$ are shown in table 5.3. In Fig. 5.2c, the magnitude of $\Delta I_{op1} < max(\Delta I_1, \Delta I_2)$, $\Delta I_{op2} < max(\Delta I_{op1}, \Delta I_3)$ and $\Delta I_{op3} < max(\Delta I_{op2}, \Delta I_4)$ for entire time period of the fault, thus not satisfying the bus fault condition of Equation (2.9). Therefore, the bus fault output of the algorithm shown in Fig. 5.2d is set to zero, representing a line fault which is external to the

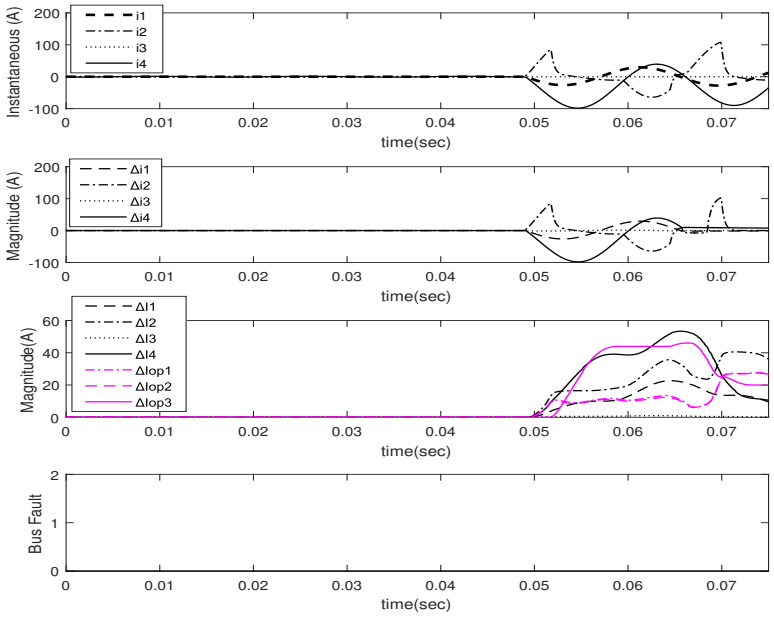

Figure 5.2: Phase-Phase to ground Line Fault with CT saturation at 49ms a. Instantaneous Current, b. Superimposed Current, c. Superimposed Current Phasor Magnitude and Superimposed POC magnitude d. Fault Discriminator

zone of protection.

Table 5.3: Phase-Phase to Ground Line Fault Superimposed Currents & SPOCs Values

At Time, t=50ms						
ΔI_1	ΔI_2	ΔI_3	ΔI_4	ΔI_{op1}	ΔI_{op2}	ΔI_{op3}
0.4904	1.5963	0.1164	0.9908	1.1059	0.9899	0.0009
$\angle 173.531°$	$\angle -6.20°$	$\angle 169.91°$	$\angle 174.39°$	$\angle -6.08°$	$\angle -5.61°$	$\angle -175.38°$

5.1.2.3 Phase-Phase Bus fault

Fig. 5.3a shows Phase-A to Phase-B bus fault at bus-1. The fault impedance was Z_f= 0.1 Ω. Fig. 5.3b shows superimposed instantaneous current at each terminal ($\Delta i_1, \Delta i_2, \Delta i_3, \Delta i_4$). The magnitude of superimposed terminal currents ($\Delta I_1, \Delta I_2, \Delta I_3, \Delta I_4$) and superimposed POCs ($\Delta I_{op1}, \Delta I_{op2}, \Delta I_{op3}$) are shown in fig. 5c. From fig. 5.3c, the magnitudes of

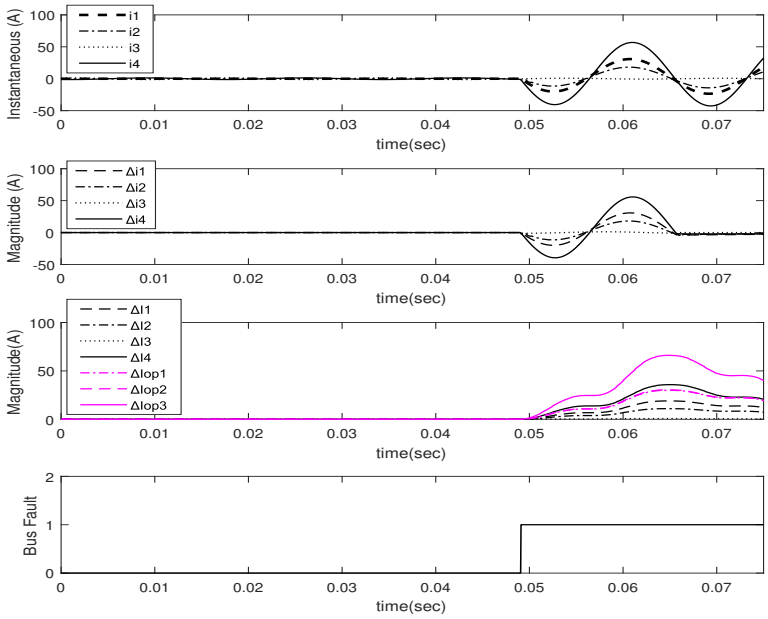

Figure 5.3: Phase-Phase Bus Fault at 49 ms a. Instantaneous Current b. Superimposed Current, c. Superimposed Current Phasor Magnitude and Superimposed POC magnitude d. Fault Discriminator

superimposed terminal currents and superimposed POCs satisfy bus fault condition of (3.3). The fault was initiated at 49 ms and fault was detected as bus fault within 0.15 ms after the fault inception. The values of $\Delta I_1, \Delta I_2, \Delta I_3, \Delta I_4, \Delta I_{op1}, \Delta I_{op2}, \Delta I_{op3}$ at t= 49.15 ms are shown in table 5.4. The magnitude of superimposed terminal current (ΔI_1, $\Delta I_2, \Delta I_3, \Delta I_4$) and superimposed POCs (ΔI_{op1}, $\Delta I_{op2}, \Delta I_{op3}$) satisfy the bus fault condition (3.3) and hence the bus fault is set to 1 by the algorithm as shown in Fig. 5.3d confirming that there is a bus fault.

Table 5.4: Phase-Phase Bus Fault Superimposed Currents & SPOCs Values

At Time, t=49.15ms						
ΔI_1	ΔI_2	ΔI_3	ΔI_4	ΔI_{op1}	ΔI_{op2}	ΔI_{op3}
0.0311	0.0308	0.0163	0.0144	0.0618	0.0781	0.09424
$\angle 161.11°$	$\angle 160.99°$	$\angle 155.32°$	$\angle 168.19°$	$\angle 161.05°$	$\angle 159.86°$	$\angle 161.15°$

5.1.2.4 Phase-Phase to Ground Bus Fault

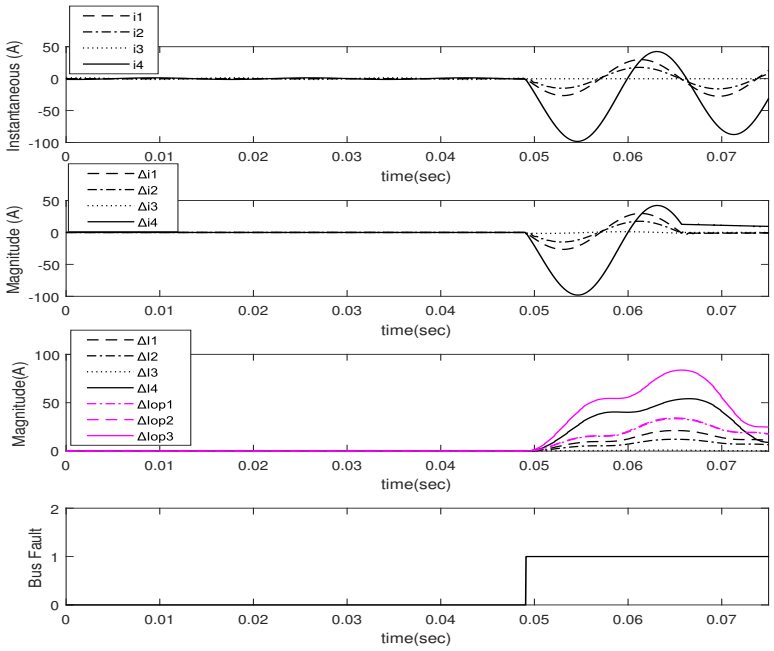

Figure 5.4: Phase-Phase to Ground Bus Fault at 49 ms a. Instantaneous Current b. Superimposed Current, c. Superimposed Current Phasor Magnitude and Superimposed POC magnitude d. Fault Discriminator

Fig. 5.4a shows Phase-A to Phase-B bus fault at Bus 1. The fault impedance was Z_f= 0.1 Ω. Fig. 5.4b shows superimposed instantaneous current at each terminal ($\Delta i_1, \Delta i_2, \Delta i_3, \Delta i_4$). The magnitude of superimposed terminal currents ($\Delta I_1, \Delta I_2, \Delta I_3, \Delta I_4$) and superimposed POCs ($\Delta I_{op1}, \Delta I_{op2}, \Delta I_{op3}$) are shown in Fig. 5.4c. From Fig. 5.4c, the magnitudes of superimposed terminal currents and superimposed POCs satisfy bus fault condition of (9). The fault was initiated at 49 ms and fault was detected as bus fault within 0.15 ms after the fault inception. The values of $\Delta I_1, \Delta I_2, \Delta I_3, \Delta I_4, \Delta I_{op1}, \Delta I_{op2}, \Delta I_{op3}$ at t= 49.15 ms are shown in table 5.5. The magnitude of superimposed terminal current ($\Delta I_1, \Delta I_2, \Delta I_3, \Delta I_4$) and superimposed POCs ($\Delta I_{op1}, \Delta I_{op2}, \Delta I_{op3}$) satisfy the bus fault condition (2.9) and hence

the bus fault is set to 1 by the algorithm as shown in Fig. 5.4d confirming that there is a bus fault.

Table 5.5: Phase-Phase to ground Bus Fault Superimposed Currents & SPOCs Values

At Time, t=49.15ms						
ΔI_1	ΔI_2	ΔI_3	ΔI_4	ΔI_{op1}	ΔI_{op2}	ΔI_{op3}
0.0330	0.0326	0.0178	0.0171	0.0655	0.0832	0 .1002
$\angle 161.11°$	$\angle 161°$	$\angle 155.80°$	$\angle 167.09°$	$\angle 161.06°$	$\angle 159.94°$	$\angle 161.15°$

5.1.3 Compare SPOC Method with POC Method

Table 5.6: 4-bus Test system SPOC Vs POC Test Cases & Results

Fault	Location	Z_f	Time(ms)			System Response	
		(Ω)	Inception	Detection Delay		SPOC	POC
				SPOC	POC		
AB	Terminal 2	0.1	49	NA	NA	Line Fault	Line Fault
AB	Terminal 2	5	49	NA	NA	Line Fault	Line Fault
AB	Terminal 2	10	49	NA	NA	Line Fault	Line Fault
AG	Terminal 2	0.1	49	NA	NA	Line Fault	Line Fault
AG	Terminal 2	5	49	NA	NA	Line Fault	Line Fault
AG	Terminal 2	10	49	NA	NA	Line Fault	Line Fault
ABG	Terminal 2	0.1	49	NA	NA	Line Fault	Line Fault
ABG	Terminal 2	5	49	NA	NA	Line Fault	Line Fault
ABG	Terminal 2	10	49	NA	NA	Line Fault	Line Fault
AB	Bus 1	0.1	49	0.15	8.9	BusFault	Bus Fault
AB	Bus 1	5	49	0.15	9.11	Bus Fault	Bus Fault
AB	Bus 1	10	49	0.15	9.43	Bus Fault	Bus Fault
ABG	Bus 1	0.1	49	0.15	8.91	Bus Fault	Bus Fault
ABG	Bus 1	5	49	0.15	9.13	Bus Fault	Bus Fault
ABG	Bus 1	10	49	0.15	9.47	Bus Fault	Bus Fault
AG	Bus 1	0.1	49	0.15	8.91	Bus Fault	Bus Fault
AG	Bus 1	5	49	0.15	9.13	Bus Fault	Bus Fault
AG	Bus 1	50	49	0.15	11.64	Bus Fault	Bus Fault
AG	Bus 1	100	49	0.15	14.30	Bus Fault	Bus Fault
AG	Bus 1	200	49	0.15	15.71	Bus Fault	Bus Fault

The performance of the POC method [5, 6] and SPOC method for various fault cases are listed in Table 5.6. Both POC and SPOC method are tested with the same 4-bus test system present in [5, 6, 15] and the respective algorithm is implemented in MATLAB. The different types of bus faults and line faults like phase to phase, phase-phase to ground, and phase to ground, with various fault impedances and locations, are tested and reported in Table 5.6. Fault is induced at 49 ms for every test case for both methods. The timing of fault detection for every bus fault is shown in Table 5.6. NA represents the test cases that the algorithm does not detect bus faults because the faults are external from the viewpoint of the bus. SPOC method accurately discriminates line faults and bus faults similar to the POC method [5, 6] as seen in Table 5.6. The speed of detecting the bus faults is faster in SPOC method than the POC method as seen in Table 5.6. The proposed SPOC method is accurate because the method discriminates bus faults from line faults in all of the test cases with no error. Comparing with the POC method, the SPOC method detects bus faults faster in every bus fault case including severe CT saturation and high impedance faults.

Time required for superimposed method to subtract present signals from one time period before signals needs to be accounted. Also, sampling time and superimposed calculation when done in a relay may take a few milliseconds would need to be accounted for. Therefore, the Detection Delay in Table 5.7 would be realistically a few milliseconds more than it is shown in the table.

5.2 IEEE 14-bus Test System

5.2.1 Test Cases

Table 5.7: Test Cases IEEE 14-bus System

Fault	Location	Z_f	Time(ms)		System Response
		(Ω)	Inception	Detection Delay	
AB	Terminal Btw Bus 1 & 2	0.1	49	NA	Line Fault
AB	Terminal Btw Bus 1 & 2	5	49	NA	Line Fault
AB	Terminal Btw Bus 1 & 2	10	49	NA	Line Fault
AG	Terminal Btw Bus 1 & 2	0.1	49	NA	Line Fault
AG	Terminal Btw Bus 1 & 2	5	49	NA	Line Fault
AG	Terminal Btw Bus 1 & 2	10	49	NA	Line Fault
ABG	Terminal Btw Bus 1 & 2	0.1	49	NA	Line Fault
ABG	Terminal Btw Bus 1 & 2	5	49	NA	Line Fault
ABG	Terminal Btw Bus 1 & 2	10	49	NA	Line Fault
AB	Bus 1	0.1	49	0.15	Bus Fault
AB	Bus 1	5	49	0.15	Bus Fault
AB	Bus 1	10	49	0.15	Bus Fault
ABG	Bus 1	0.1	49	0.15	Bus Fault
ABG	Bus 1	5	49	0.15	Bus Fault
ABG	Bus 1	10	49	0.15	Bus Fault
AG	Bus 1	0.1	49	0.15	Bus Fault
AG	Bus 1	5	49	0.15	Bus Fault
AG	Bus 1	50	49	0.15	Bus Fault
AG	Bus 1	100	49	0.15	Bus Fault
AG	Bus 1	200	49	0.15	Bus Fault

The performance of the proposed method for various fault cases are listed in Table 5.7. Z_f represents the fault impedance. The different types of bus faults and line faults like Phase to Phase, Phase-Phase to ground, and Phase to ground, with various fault impedances and locations, are tested and reported in Table 5.7. Fault is induced at 49 ms for every test case. The timing of fault detection for every bus fault is shown in Table 5.7. NA represents the

test cases that the algorithm does not detect bus faults because the faults are external from the view point of bus. The proposed method is fast with the fault detection within 0.15 ms after fault inception. The method accurately discriminates bus faults and line faults for all test cases shown in Table 5.7 including various severe CT saturation and high impedance faults. For example, a bus fault of high impedance Z_f= 200 Ω is detected successfully by the method within 0.15 ms time.

5.2.2 Discussion of Results

Only four of the key fault cases is explained in the following subsection. The results of all the test cases in Table 5.7 are included in Appendix A.2.

5.2.2.1 Phase to Ground Line Fault with CT Saturation

Fig. 5.5a shows Phase to Ground line fault at terminal between bus-1 & bus-2. which caused i_2 terminal to get distorted because of CT saturation. The fault impedance was Z_f= 0.1 Ω. Fig. 5.5b shows superimposed instantaneous current ($\Delta i_1, \Delta i_2, \Delta i_3$) values. The magnitude of superimposed terminal currents ($\Delta I_1, \Delta I_2, \Delta I_3$) and superimposed POCs ($\Delta I_{op1}, \Delta I_{op2}$) are shown in Fig. 5.5c. At time $t = 50ms$ in Fig. 5.5c, the values of $\Delta I_1, \Delta\ I_2, \Delta I_3, \Delta I_{op1}, \Delta I_{op2}$ are shown in Table 5.8. In Fig. 5.5c, the magnitude of $\Delta I_{op1} < max(\Delta I_1, \Delta I_2)$ and $\Delta I_{op2} < max(\Delta I_{op1}, \Delta I_3)$ for entire time period of the fault, thus not satisfying the bus fault condition of Equation (3.3). Therefore, the bus fault output of the algorithm shown in Fig. 5.5d is set to zero, representing a line fault which is external to the zone of protection.

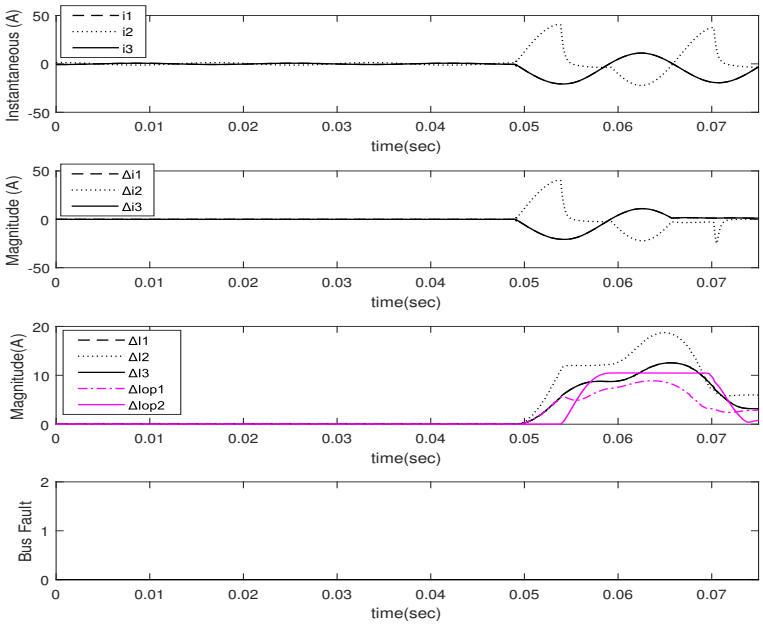

Figure 5.5: Phase to Ground Line Fault with CT saturation at 49ms a. Instantaneous Current, b. Superimposed Current, c. Superimposed Current Phasor Magnitude and Superimposed POC magnitude d. Fault Discriminator

Table 5.8: Phase to Ground Line Fault Superimposed Currents & SPOCs Values

At Time, t=50ms				
ΔI_1	ΔI_2	ΔI_3	ΔI_{op1}	ΔI_{op2}
0.2947	0.5889	0.2947	0.2943	0.0004
$\angle 174.29°$	$\angle -5.71°$	$\angle 174.29°$	$\angle -5.71°$	$\angle 179.07°$

5.2.2.2 Phase-Phase to Ground Line Fault with CT Saturation

Fig. 5.6a shows Phase to Ground line fault at terminal between bus-1 & bus-2. which caused i_2 terminal to get distorted because of CT saturation. The fault impedance was Z_f= 0.1 Ω. Fig. 5.6b shows superimposed instantaneous current $(\Delta i_1, \Delta i_2, \Delta i_3)$ values. The magnitude of superimposed terminal currents $(\Delta I_1, \Delta I_2, \Delta I_3)$ and superimposed POCs $(\Delta I_{op1}, \Delta I_{op2})$ are shown in Fig. 5.6c. At time $t = 50ms$ in Fig. 5.5c, the values of $\Delta I_1, \Delta\ I_2, \Delta I_3, \Delta I_{op1}, \Delta I_{op2}$

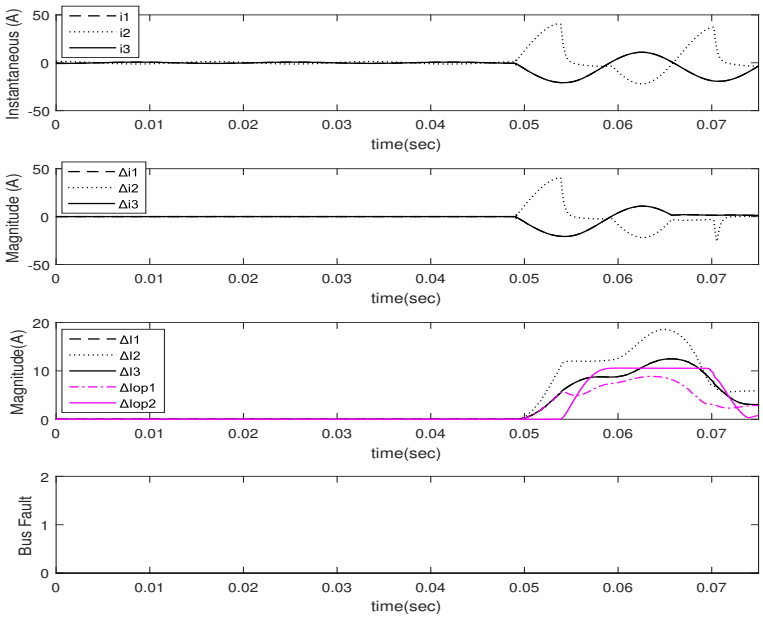

Figure 5.6: Phase-Phase to ground Line Fault with CT saturation at 49ms a. Instantaneous Current, b. Superimposed Current, c. Superimposed Current Phasor Magnitude and Superimposed POC magnitude d. Fault Discriminator

are shown in Table 5.9. In Fig. 5.6c, the magnitude of $\Delta I_{op1} < max(\Delta I_1, \Delta I_2)$ and $\Delta I_{op2} < max(\Delta I_{op1}, \Delta I_3)$ for entire time period of the fault, thus not satisfying the bus fault condition of Equation (3.3). Therefore, the bus fault output of the algorithm shown in Fig. 5.6d is set to zero, representing a line fault which is external to the zone of protection.

Table 5.9: Phase-Phase to Ground Line Fault Superimposed Currents & SPOCs Values

At Time, t=50ms

ΔI_1	ΔI_2	ΔI_3	ΔI_{op1}	ΔI_{op2}
0.2929	0.5854	0.2929	0.2925	0.0004
$\angle 174.28°$	$\angle -5.73°$	$\angle 174.28°$	$\angle -5.73°$	$\angle 179.07°$

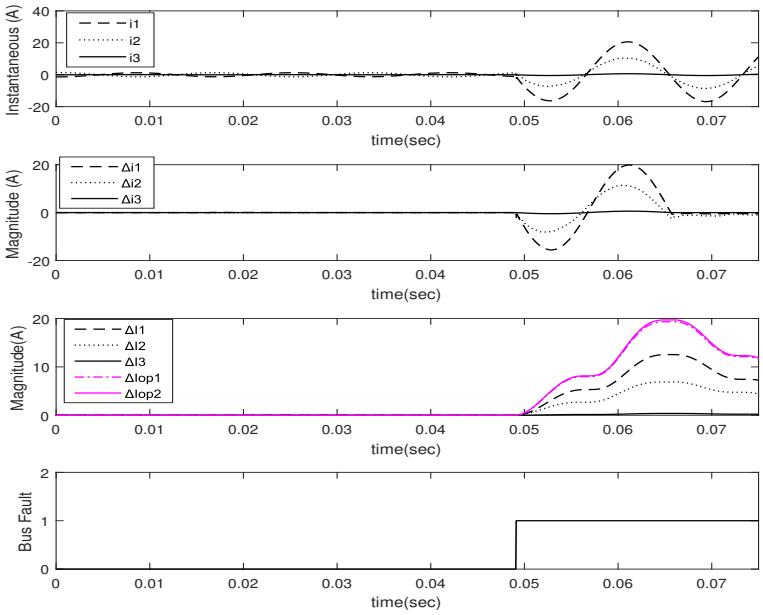

Figure 5.7: Phase to Ground Bus Fault at 49 ms a. Instantaneous Current b. Superimposed Current, c. Superimposed Current Phasor Magnitude and Superimposed POC magnitude d. Fault Discriminator

5.2.2.3 Phase to Ground Bus Fault

Fig. 5.7a shows phase-A to ground bus fault at bus-1. The fault impedance was Z_f= 0.1 Ω. Fig. 5.7b shows superimposed instantaneous current at each terminal ($\Delta i_1, \Delta i_2, \Delta i_3$). The magnitude of superimposed terminal currents ($\Delta I_1, \Delta I_2, \Delta I_3$,) and superimposed POCs ($\Delta I_{op1}, \Delta I_{op2}$) are shown in Fig. 5.7c. From Fig. 5.7c, the magnitudes of superimposed terminal currents and superimposed POCs satisfy bus fault condition of (3.3). The fault was initiated at 49 ms and fault was detected as bus fault within 0.15 ms after the fault inception. The values of $\Delta I_1, \Delta I_2, \Delta I_3, \Delta I_{op1}$, ΔI_{op2} at t= 49.15 ms are shown in Table 5.10. The magnitude of superimposed terminal current (ΔI_1, $\Delta I_2, \Delta I_3$) and superimposed POCs (ΔI_{op1}, ΔI_{op2}) satisfy the bus fault condition (3.3) and hence the bus fault is set to 1 by the

algorithm as shown in Fig. 5.7d confirming that there is a bus fault.

Table 5.10: Phase to Ground Bus Fault Superimposed Currents & SPOCs Values

At Time, t=49.15ms				
ΔI_1	ΔI_2	ΔI_3	ΔI_{op1}	ΔI_{op2}
0.0313	0.033	0.0009	0.0641	0.065
$\angle 157.33°$	$\angle 165.10°$	$\angle 157.33°$	$\angle 161.32°$	$\angle 161.26°$

5.2.2.4 Phase-Phase to Ground Bus Fault

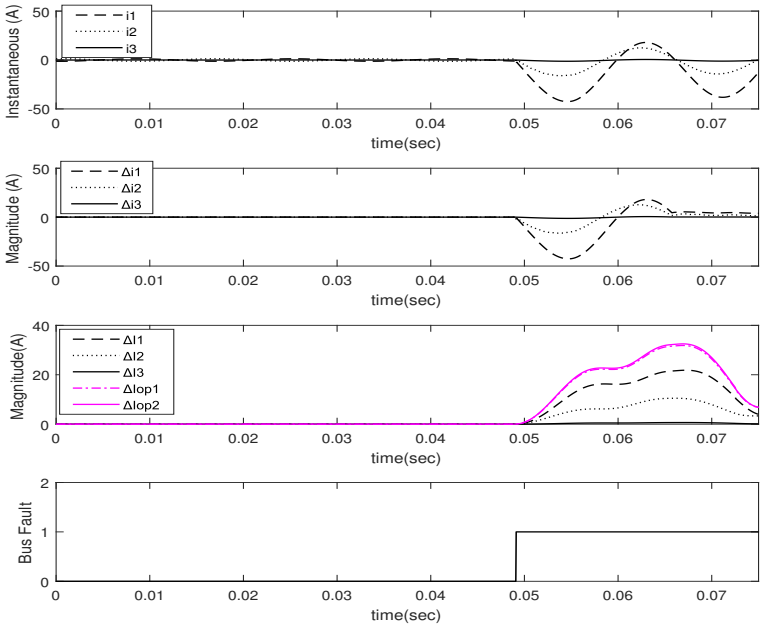

Figure 5.8: Phase-Phase to Ground Bus Fault at 49 ms a. Instantaneous Current b. Superimposed Current, c. Superimposed Current Phasor Magnitude and Superimposed POC magnitude d. Fault Discriminator

Fig. 5.8a shows phase-A to ground bus fault at bus-1. The fault impedance was Z_f= 0.1 Ω. Fig. 5.8b shows superimposed instantaneous current at each terminal ($\Delta i_1, \Delta i_2, \Delta i_3$). The magnitude of superimposed terminal currents ($\Delta I_1, \Delta I_2, \Delta I_3$,) and superimposed POCs

($\Delta I_{op1}, \Delta I_{op2}$) are shown in Fig. 5.8c. From Fig. 5.8c, the magnitudes of superimposed terminal currents and superimposed POCs satisfy bus fault condition of (3.3). The fault was initiated at 49 ms and fault was detected as bus fault within 0.15 ms after the fault inception. The values of $\Delta I_1, \Delta I_2, \Delta I_3, \Delta I_{op1}$, ΔI_{op2} at t= 49.15 ms are shown in Table 5.11. The magnitude of superimposed terminal current (ΔI_1, $\Delta I_2, \Delta I_3$) and superimposed POCs (ΔI_{op1}, ΔI_{op2}) satisfy the bus fault condition (3.3) and hence the bus fault is set to 1 by the algorithm as shown in Fig. 5.8d confirming that there is a bus fault.

Table 5.11: Phase-Phase to ground Bus Fault Superimposed Currents & SPOCs Values

At Time, t=49.15ms				
ΔI_1	ΔI_2	ΔI_3	ΔI_{op1}	ΔI_{op2}
0.0295	0.0330	0.0008	0.0623	0.0632
$\angle 157.06°$	$\angle 165.09°$	$\angle 157.06°$	$\angle 161.31°$	$\angle 161.25°$

5.2.3 Compare SPOC Method with POC Method

The performance of the POC method [5, 6] and SPOC method for various fault cases are listed in Table 5.12. Both POC and SPOC method are tested using the same 14-bus test system [22, 23] and the respective algorithm implemented in MATLAB. The different types of bus faults and line faults like phase to phase, phase-phase to ground, and phase to ground, with various fault impedances and locations, are tested and reported in Table 5.12. Fault is induced at 49 ms for every test case for both methods. The timing of fault detection for every bus fault is shown in Table 5.12. NA represents the test cases that the algorithm does not detect bus faults because the faults are external from the viewpoint of the bus. SPOC method accurately discriminates line faults and bus faults similar to the POC method [5, 6]

Table 5.12: IEEE 14-bus Test system SPOC Vs POC Test Cases & Results

Fault	Location	Z_f (Ω)	Time(ms)			System Response	
			Inception	Detection Delay SPOC	Detection Delay POC	SPOC	POC
AB	Terminal Btw Bus 1 & 2	0.1	49	NA	NA	Line Fault	Line Fault
AB	Terminal Btw Bus 1 & 2	5	49	NA	NA	Line Fault	Line Fault
AB	Terminal Btw Bus 1 & 2	10	49	NA	NA	Line Fault	Line Fault
AG	Terminal Btw Bus 1 & 2	0.1	49	NA	NA	Line Fault	Line Fault
AG	Terminal Btw Bus 1 & 2	5	49	NA	NA	Line Fault	Line Fault
AG	Terminal Btw Bus 1 & 2	10	49	NA	NA	Line Fault	Line Fault
ABG	Terminal Btw Bus 1 & 2	0.1	49	NA	NA	Line Fault	Line Fault
ABG	Terminal Btw Bus 1 & 2	5	49	NA	NA	Line Fault	Line Fault
ABG	Terminal Btw Bus 1 & 2	10	49	NA	NA	Line Fault	Line Fault
AB	Bus 1	0.1	49	0.15	8.87	Bus Fault	Bus Fault
AB	Bus 1	5	49	0.15	9.11	Bus Fault	Bus Fault
AB	Bus 1	10	49	0.15	9.43	Bus Fault	Bus Fault
ABG	Bus 1	0.1	49	0.15	8.91	Bus Fault	Bus Fault
ABG	Bus 1	5	49	0.15	9.13	Bus Fault	Bus Fault
ABG	Bus 1	10	49	0.15	9.47	Bus Fault	Bus Fault
AG	Bus 1	0.1	49	0.15	8.91	Bus Fault	Bus Fault
AG	Bus 1	5	49	0.15	9.13	Bus Fault	Bus Fault
AG	Bus 1	50	49	0.15	11.64	Bus Fault	Bus Fault
AG	Bus 1	100	49	0.15	14.30	Bus Fault	Bus Fault
AG	Bus 1	200	49	0.15	15.71	Bus Fault	Bus Fault

as seen in Table 5.12. The speed of detecting the bus faults is faster in SPOC method then POC method as seen in Table 5.12. Thus, analyzing table 5.12, the proposed SPOC method is accurate and fast to detect the fault including severe CT saturation and high impedance fault.

As discussed in Section 5.1, time required for superimposed method to subtract present signals from one time period before signals needs to be accounted. Also, sampling time and superimposed calculation when done in a relay may take a few milliseconds would need to be accounted for. Therefore, the Detection Delay in Table 5.7 would be realistically a few milliseconds more than it is shown in the table.

Chapter 6

Conclusion and Future Works

This chapter provides the conclusive remark of the study conducted in this thesis based on [15]. The development of new technique Superimposed Partial Operating Current (SPOC) in directional comparison bus protection and the comparison of the SPOC method [15] with the POC method [5, 6] are presented in this thesis. The possibility of the future works that can be continued are explained in this chapter.

6.1 Conclusion

Thesis presents a new technique in directional comparison bus protection which modifies the POC method [5, 6] by using superimposed current implemented in the time-domain superimposed method to detect faults without the use of CVTs. 4-bus test system and IEEE 14-bus test system used to validate the proposed method were simulated in EMTP and the proposed algorithm was implemented in MATLAB subjected to various fault cases including severe CT saturation and high impedance. All the test cases that represent bus faults satisfy the SPOC bus fault condition of equation (3.3) and all cases representing line faults violate the superimposed bus fault condition (3.3). The proposed method is solely based on instantaneous subtraction and vector addition, hence computational burden is

less than other existing directional methods that require vector multiplication and division. Detecting bus faults by the proposed method is very fast and accurate for various fault cases including severe CT saturation and high impedance fault cases.

6.2 Future Works

This work can be continued by comparing the performance of the proposed method with other existing directional comparison methods such as time-domain superimposed directional element and voltage polarized directional element methods. The comparison will help to compare the increase in the speed and accuracy of SPOC that does not need CVTs with other directional comparison methods. For the existing directional methods, the system simulations would need to capture both voltage and current signals because the methods requires CVTs to detect faults. While both 4-bus and IEEE 14-bus test systems used in this thesis indicate that the proposed SPOC method performs really well, the author would recommend testing the proposed method further using larger scale test systems such as IEEE 39-bus, IEEE 57-bus, IEEE 118-bus test systems, in order to capture the performance and sensitivity of the SPOC algorithm to a more realistic power system.

Bibliography

[1] L. Hewitson, M. Brown, and R. Balakrishnan in *Practical Power System Protection* (L. Hewitson, M. Brown, and R. Balakrishnan, eds.), pp. 1 – 4, Oxford: Newnes, 2005.

[2] M. R. D. Zadeh, T. S. Sidhu, and A. Klimek, "Suitability analysis of practical directional algorithms for use in directional comparison bus protection based on iec61850 process bus," *IET Generation, Transmission Distribution*, vol. 5, pp. 199–208, February 2011.

[3] R. Hughes and E. Legrand, "Numerical busbar protection benefits of numerical technology in electrical substation," in *2001 Seventh International Conference on Developments in Power System Protection (IEE)*, pp. 463–466, 2001.

[4] H. S. Gill, T. S. Sidhu, and M. S. Sachdev, "Microprocessor-based busbar protection system," *IEE Proceedings - Generation, Transmission and Distribution*, vol. 147, pp. 252–260, Jul 2000.

[5] M. Hossain, I. Leevongwat, and P. Rastgoufard, "Partial operating current characteristics to discriminate internal and external faults of differential protection zones during ct saturation," *IET Generation, Transmission Distribution*, vol. 12, no. 2, pp. 379–387, 2018.

[6] M. Hossain, I. Leevongwat, and P. Rastgoufard, "Design and testing of a bus differential protection scheme using partial operating current (poc) algorithm," *Electric Power Systems Research*, vol. 157, pp. 29 – 38, 2018.

[7] "Discussion on 'busbar protection: a critical review of methods and practice' at a joint meeting of the measurements section and the transmission section, 19th february, 1943," *Electrical Engineers - Part II: Power Engineering, Journal of the Institution of*, vol. 90, pp. 288–303, October 1943.

[8] M. Hossain, I. Leevongwat, and P. Rastgoufard, "Fast fault detection challenge for alienation coefficient based bus fault discriminator," in *2018 71st Annual Conference for Protective Relay Engineers (CPRE)*, pp. 1–6, March 2018.

[9] M. Hossain, I. Leevongwat, and P. Rastgoufard, "Comparative analysis of fault discrimination algorithms on sensitivity to high impedance busbar faults," in *2017 North American Power Symposium (NAPS)*, pp. 1–6, Sept 2017.

[10] A. K. Pradhan, A. Routray, and S. M. Gudipalli, "Fault direction estimation in radial distribution system using phase change in sequence current," *IEEE Transactions on Power Delivery*, vol. 22, pp. 2065–2071, Oct 2007.

[11] A. F. Elneweihi, E. O. Schweitzer, and M. W. Feltis, "Negative-sequence overcurrent element application and coordination in distribution protection," *IEEE Transactions on Power Delivery*, vol. 8, pp. 915–924, July 1993.

[12] M. S. Sachdev, T. S. Sidhu, and H. S. Gill, "A busbar protection technique and its performance during ct saturation and ct ratio-mismatch," *IEEE Transactions on Power Delivery*, vol. 15, pp. 895–901, Jul 2000.

[13] G. Benmouyal and S. Chano, "Characterization of phase and amplitude comparators in uhs directional relays," *IEEE Transactions on Power Systems*, vol. 12, pp. 646–653, May 1997.

[14] P. G. McLaren, G. W. Swift, Z. Zhang, E. Dirks, R. P. Jayasinghe, and I. Fernando, "A new directional element for numerical distance relays," *IEEE Transactions on Power Delivery*, vol. 10, pp. 666–675, Apr 1995.

[15] B.Baral, I. Leevongwat, and M. Hossain, "Directional comparison bus protection using partial operating current characteristics," in *2018 IEEE Power Systems Conference*, September 2018.

[16] A. Apostolov, "Iec 61850 based bus protection - principles and benefits," in *2009 IEEE Power Energy Society General Meeting*, pp. 1–6, July 2009.

[17] M. M. Eissa, "A novel digital directional technique for bus-bars protection," *IEEE Transactions on Power Delivery*, vol. 19, pp. 1636–1641, Oct 2004.

[18] A. P. Apostolov, "High speed peer-to-peer communications based bus protection," in *2001 IEEE Power Engineering Society Winter Meeting. Conference Proceedings (Cat. No.01CH37194)*, vol. 2, pp. 693–698 vol.2, 2001.

[19] A. Apostolov, "Implementation of a transient energy method for directional detection in numerical distance relays," in *1999 IEEE Transmission and Distribution Conference (Cat. No. 99CH36333)*, vol. 1, pp. 382–387 vol.1, Apr 1999.

[20] A. P. Apostolov, D. Tholomier, and S. H. Richards, "Superimposed components based sub-cycle protection of transmission lines," in *IEEE PES Power Systems Conference and Exposition, 2004.*, pp. 592–597 vol.1, Oct 2004.

[21] D. Tholomier, S. Richardst, and A. Apostolov, "Which one is better - line differential or directional comparison?," in *2008 IET 9th International Conference on Developments in Power System Protection (DPSP 2008)*, pp. 86–91, March 2008.

[22] S. Munukuntla, "A busbar protection technique and its performance during ct saturation and ct ratio-mismatch," *University of New Orleans Theses and Dissertations. 2172*, 2016.

[23] M. Hossain, "Performance optimization of the differential protection schemes," *University of New Orleans Theses and Dissertations. 2566*, 2018.

[24] M. Hossain, "Fault discrimination algorithm for busbar differential protection relaying using partial operating current characteristics," *University of New Orleans Theses and Dissertations. 2263*, 2016.

[25] Horowitz, S.H., Phadke, and A.G., *Power system relaying.* (Research Studies Press Limited, 2008, 3rd edn.).

[26] B. Kasztenny, G. Benmouyal, Altuve, and H. et al.:, "Tutorial on operating characteristics of microprocessor-based multiterminal line current differential relays," October 2011.

[27] J. Roberts, D. Tziouvaras, G. Benmouyal, and *et al*, "The effect of multiprinciple line protection on dependability and security," in *Southern African Power System Protection Conf., November 2000*, November 2000.

[28] F. Gao and K. Strunz, "Modeling of constant distributed parameter transmission line for simulation of natural and envelope waveforms in power electric networks," in *Proceedings of the 37th Annual North American Power Symposium, 2005.*, pp. 247–252, Oct 2005.

[29] M. Kezunovic, L. Kojovic, A. Abur, C. W. Fromen, D. R. Sevcik, and F. Phillips, "Experimental evaluation of emtp-based current transformer models for protective relay transient study," *IEEE Transactions on Power Delivery*, vol. 9, pp. 405–413, Jan 1994.

Appendix A

An Appendix

A.1 Four Bus Test System Test Cases

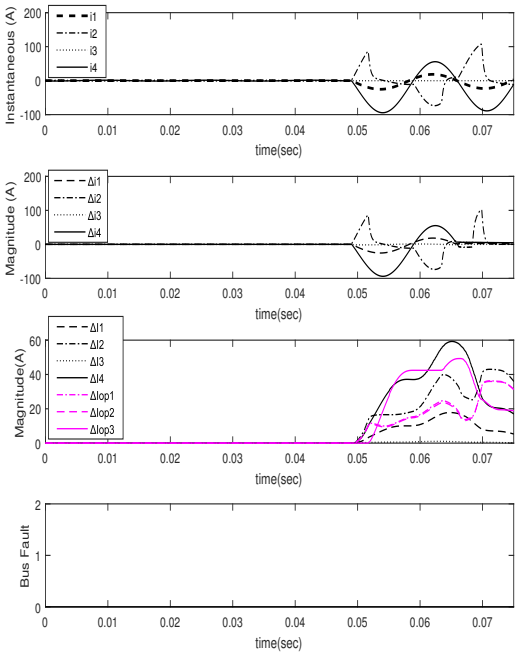

Figure A.1: Phase to ground Line Fault at 49ms, Z_f= 0.1 Ω

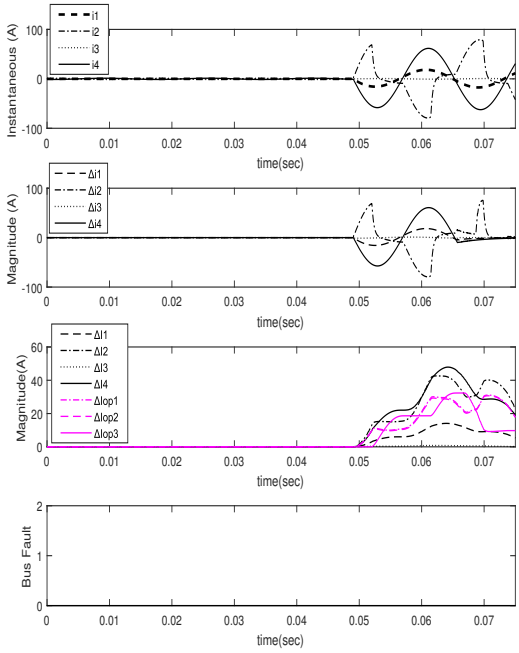

Figure A.2: Phase to ground Line Fault at 49ms, Z_f= 5 Ω

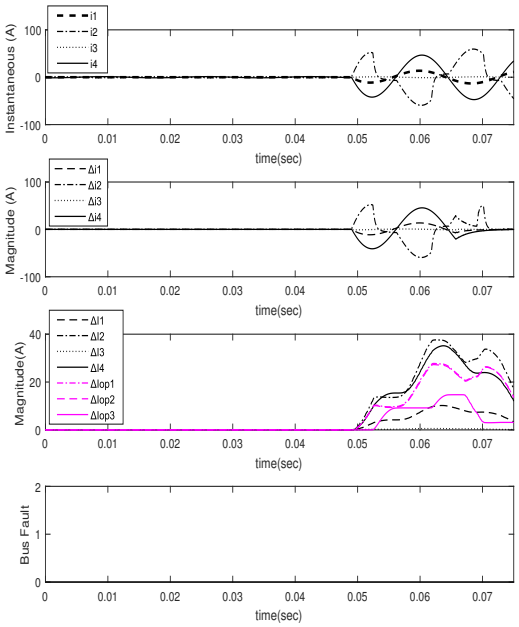

Figure A.3: Phase to ground Line Fault at 49ms, Z_f= 10 Ω

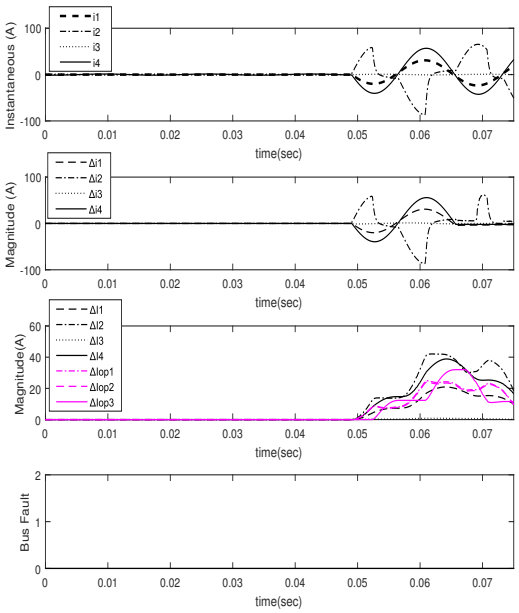

Figure A.4: Phase-Phase Line Fault at 49ms, Z_f= 0.1 Ω

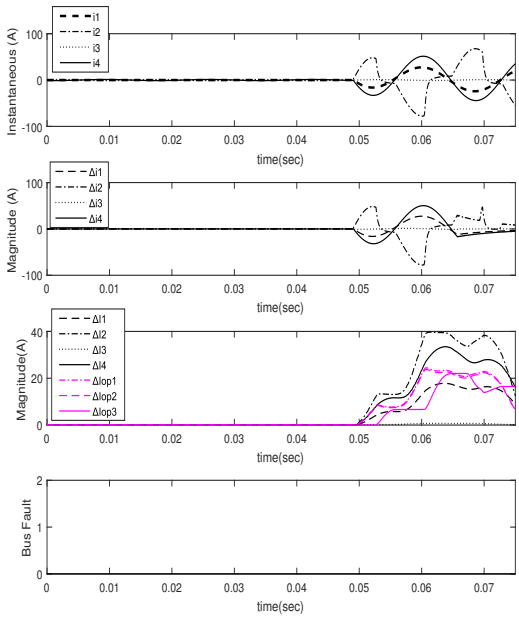

Figure A.5: Phase-Phase Line Fault at 49ms, Z_f= 5 Ω

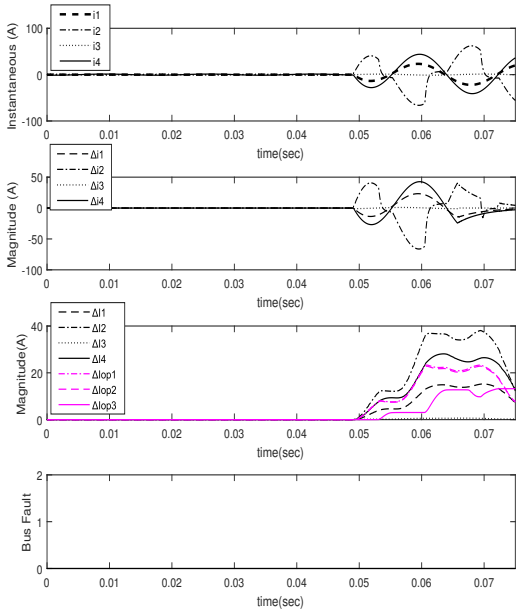

Figure A.6: Phase-Phase Line Fault at 49ms, Z_f= 10 Ω

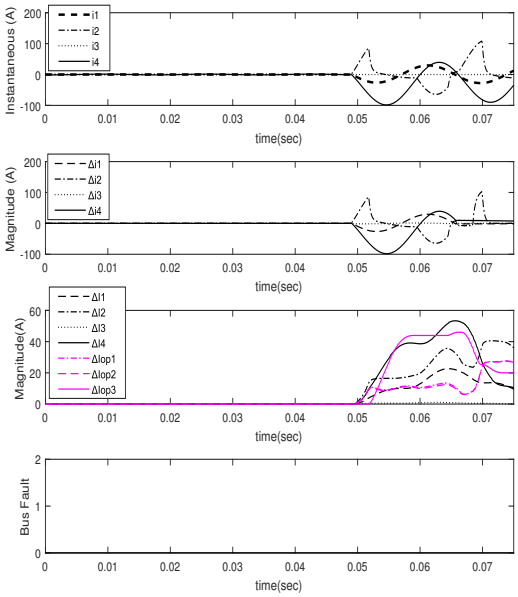

Figure A.7: Phase-Phase to ground Line Fault at 49ms, Z_f= 0.1 Ω

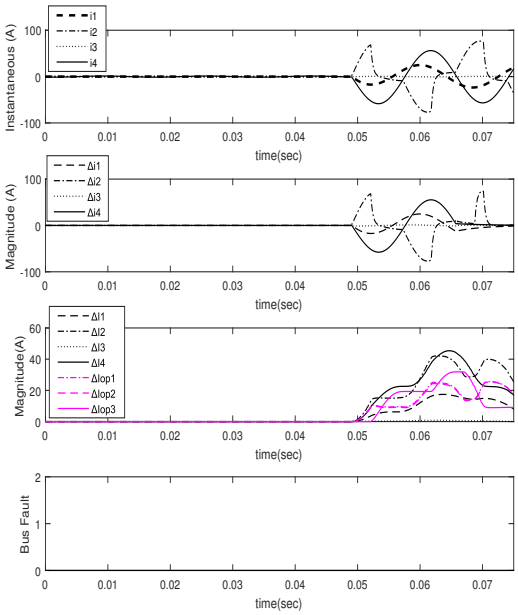

Figure A.8: Phase-Phase to ground Line Fault at 49ms, Z_f= 5 Ω

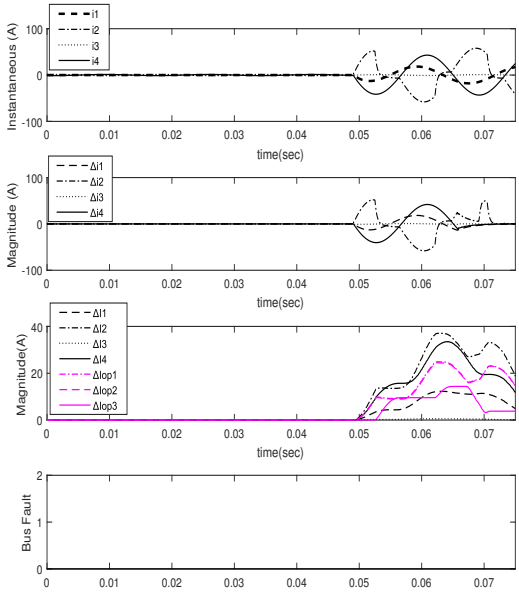

Figure A.9: Phase-Phase to ground Line Fault at 49ms, Z_f= 10 Ω

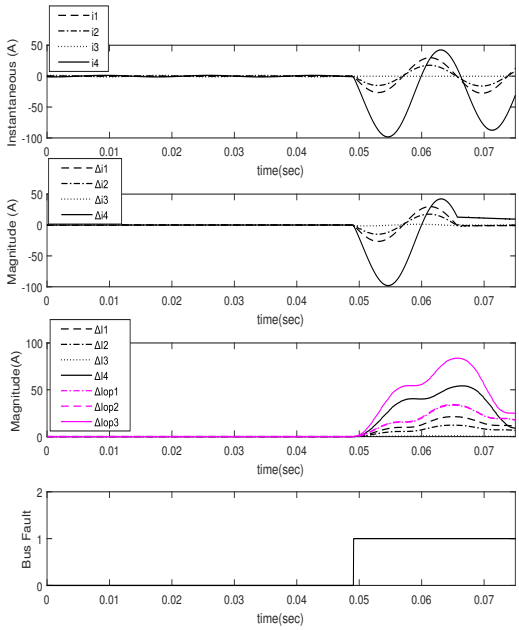

Figure A.10: Phase-Phase to ground Bus Fault at 49ms, Z_f= 0.1 Ω

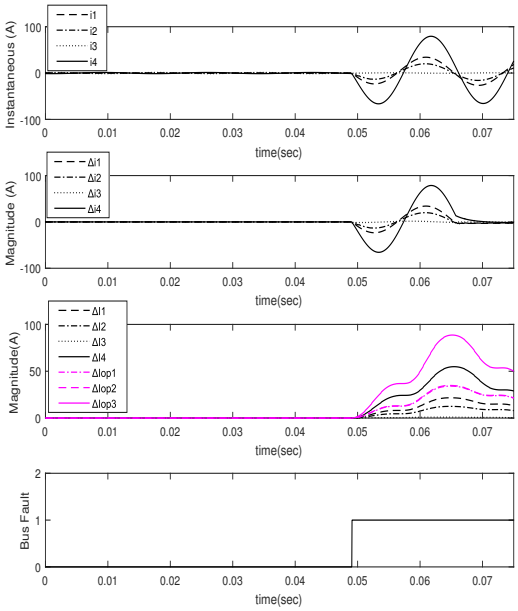

Figure A.11: Phase-Phase to ground Bus Fault at 49ms, Z_f= 5 Ω

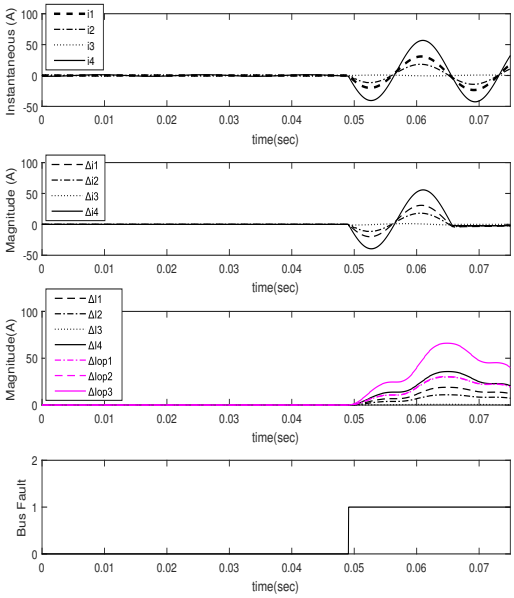

Figure A.13: Phase-Phase Bus Fault at 49ms, Z_f= 0.1 Ω

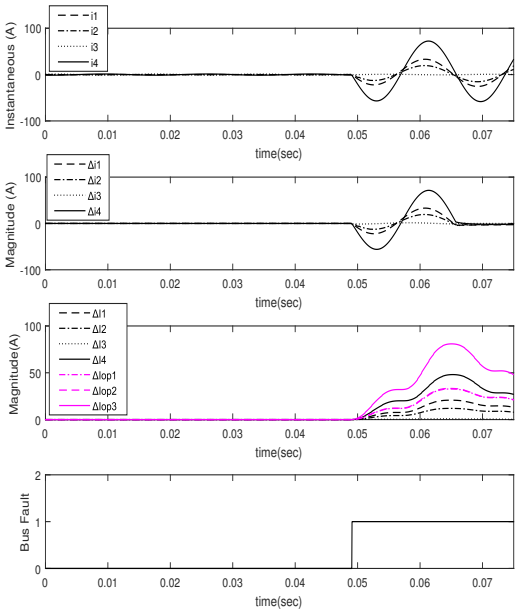

Figure A.12: Phase-Phase to ground Bus Fault at 49ms, Z_f= 10 Ω

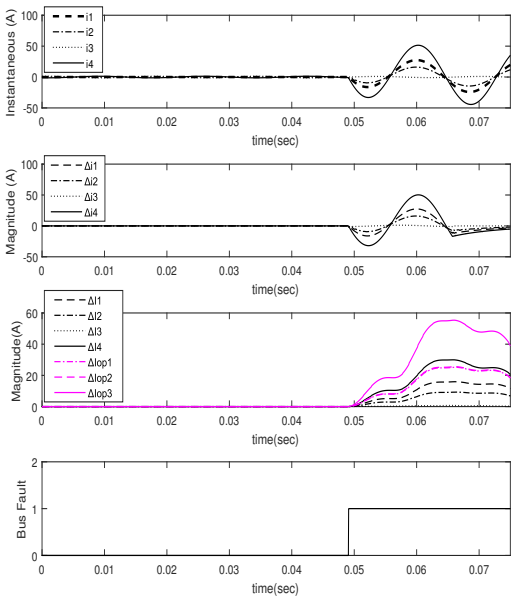

Figure A.14: Phase-Phase Bus Fault at 49ms, Z_f= 5 Ω

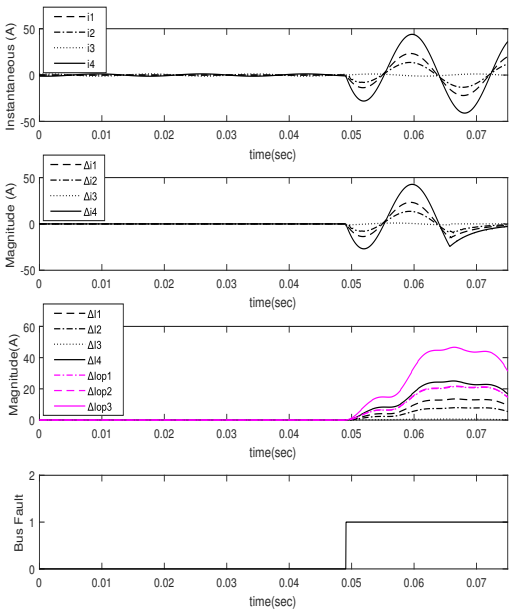

Figure A.15: Phase-Phase Bus Fault at 49ms, Z_f= 10 Ω

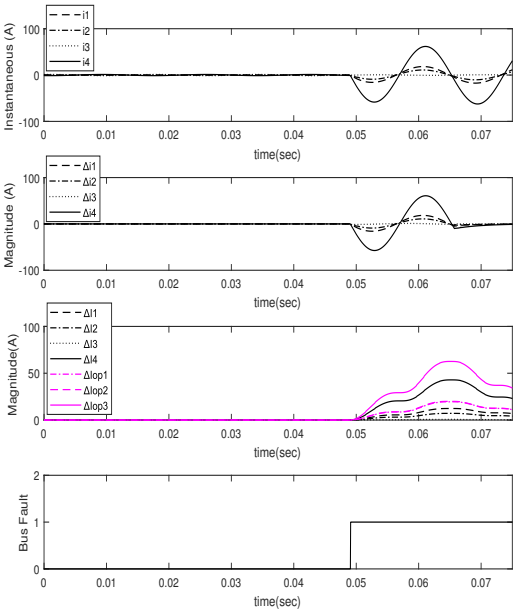

Figure A.17: Phase to ground Bus Fault at 49ms, Z_f= 5 Ω

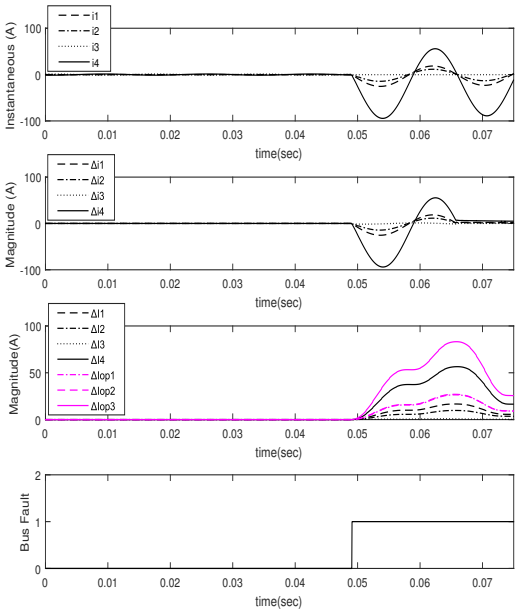

Figure A.16: Phase to ground Bus Fault at 49ms, Z_f= 0.1 Ω

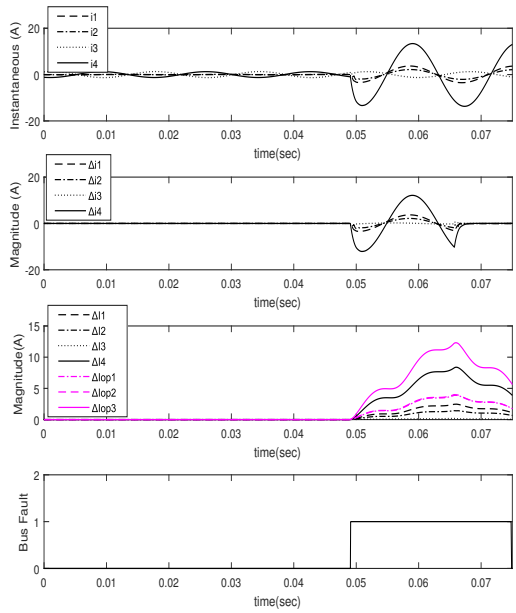

Figure A.18: Phase to ground Bus Fault at 49ms, Z_f= 50 Ω

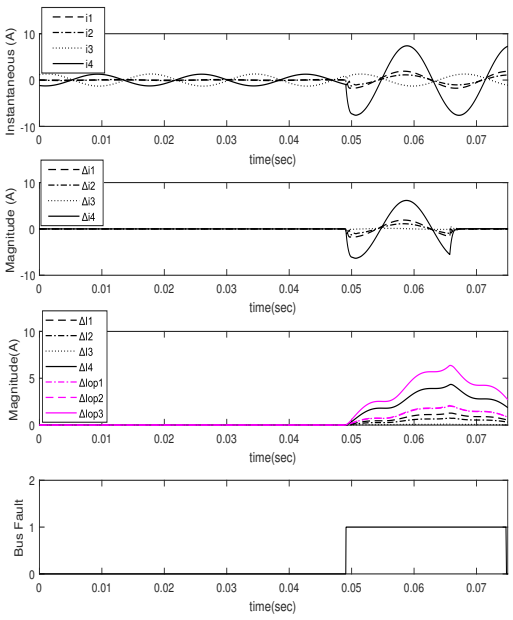

Figure A.19: Phase to ground Bus Fault at 49ms, Z_f= 100 Ω

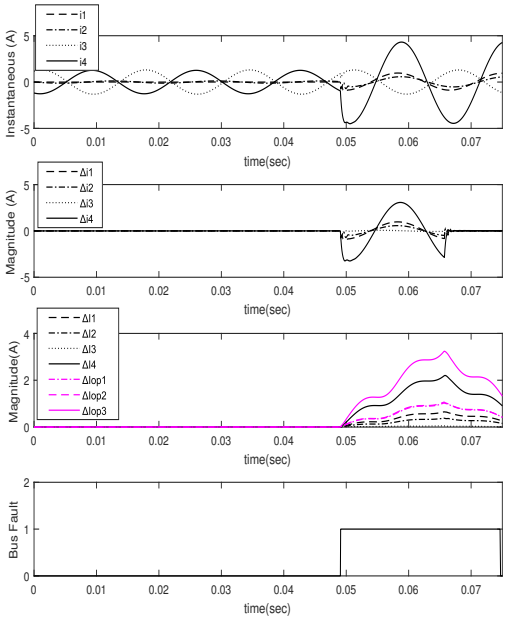

Figure A.20: Phase to ground Bus Fault at 49ms, Z_f= 200 Ω

A.2 IEEE 14-bus Test System Test Cases

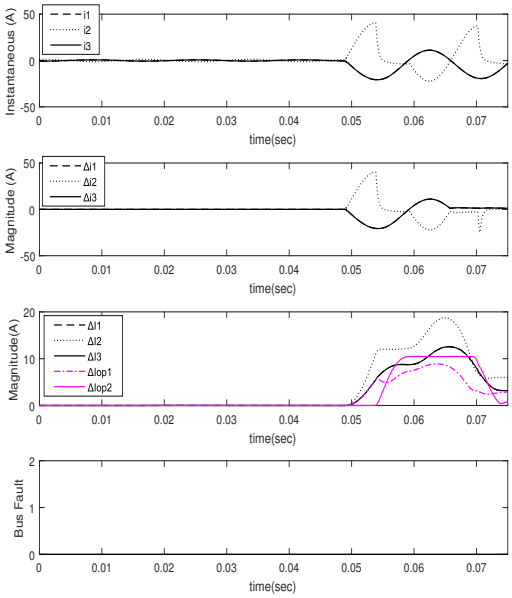

Figure A.21: Phase to ground Line Fault at 49ms, Z_f= 0.1 Ω

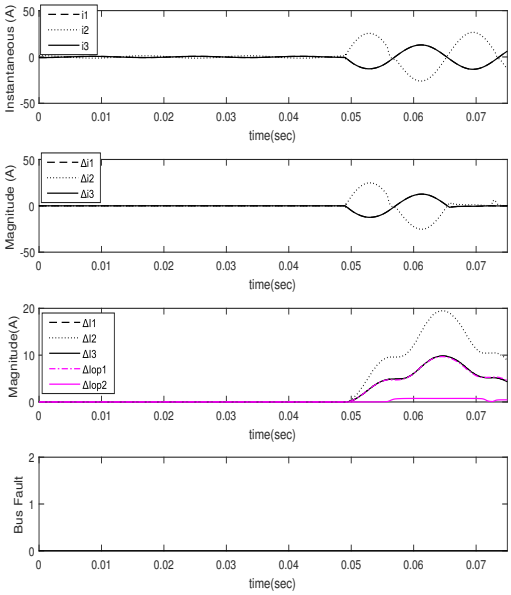

Figure A.22: Phase to ground Line Fault at 49ms, Z_f= 5 Ω

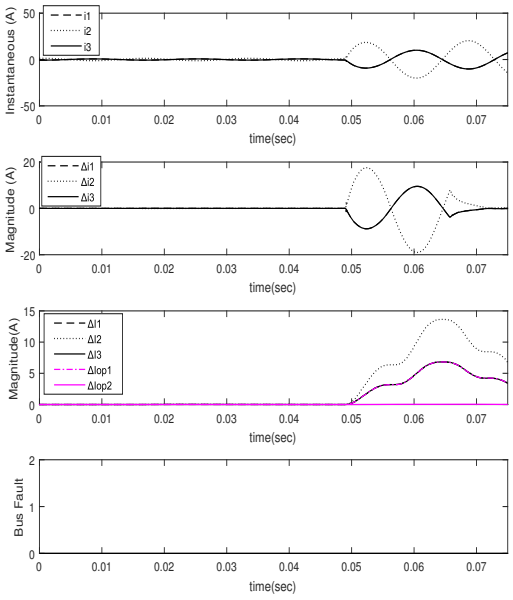

Figure A.23: Phase to ground Line Fault at 49ms, Z_f= 10 Ω

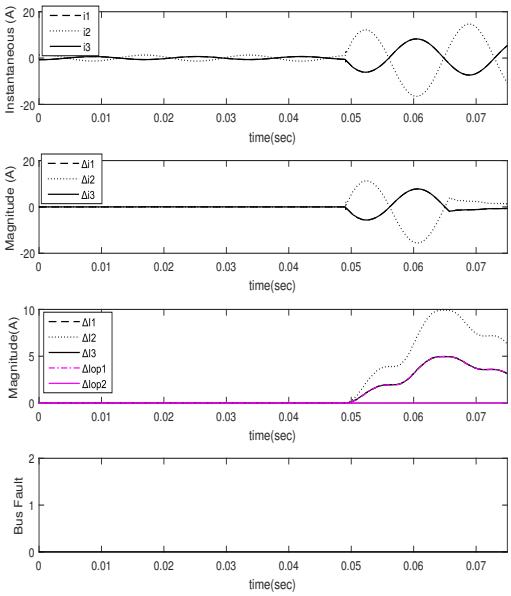

Figure A.25: Phase-Phase Line Fault at 49ms, Z_f= 5 Ω

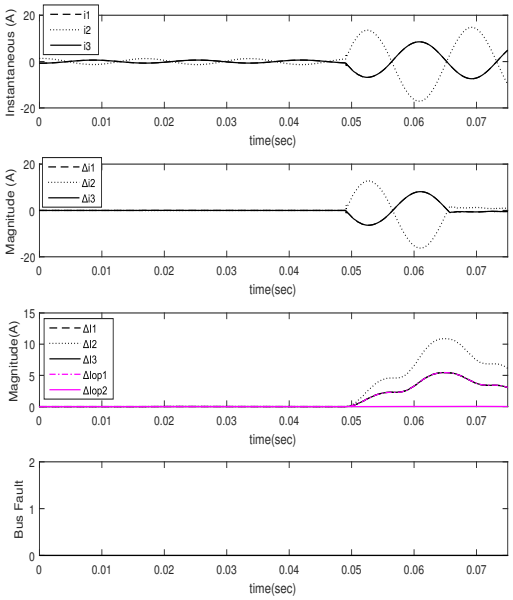

Figure A.24: Phase-Phase Line Fault at 49ms, Z_f= 0.1 Ω

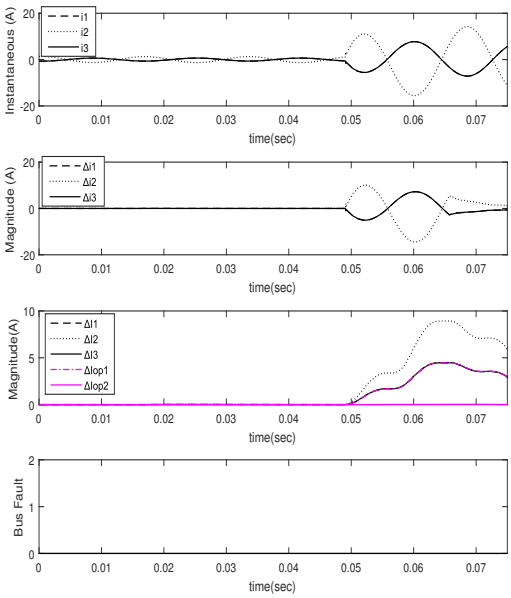

Figure A.26: Phase-Phase Line Fault at 49ms, Z_f= 10 Ω

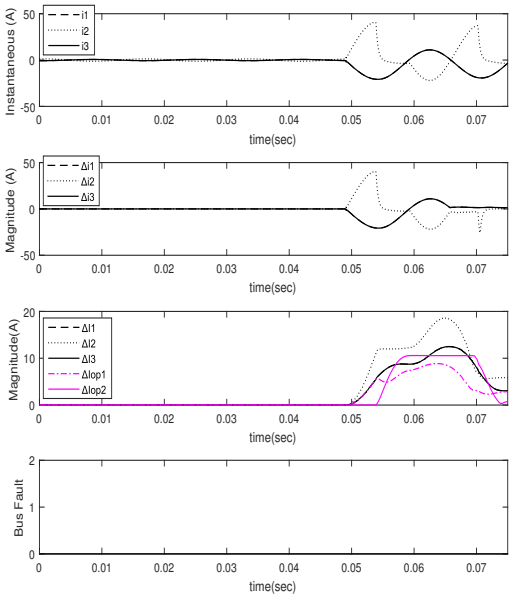

Figure A.27: Phase-Phase to ground Line Fault at 49ms, Z_f= 0.1 Ω

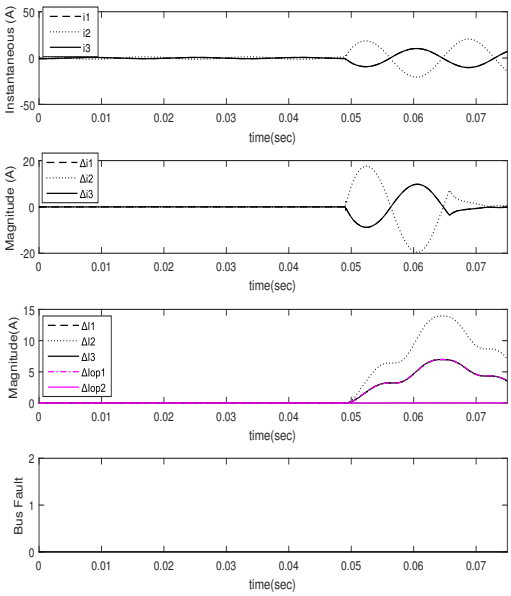

Figure A.29: Phase-Phase to ground Line Fault at 49ms, Z_f= 10 Ω

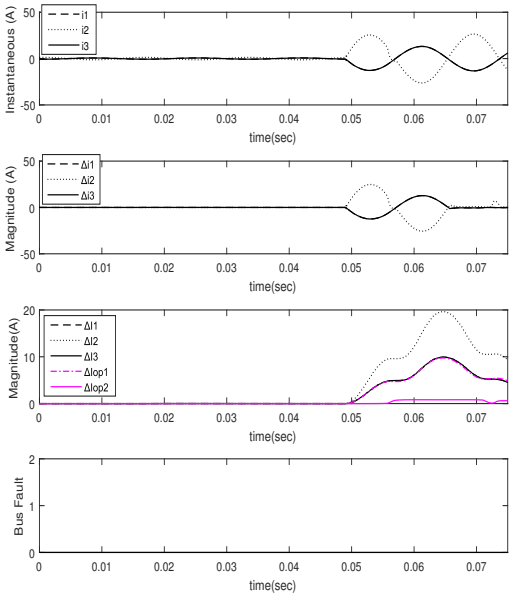

Figure A.28: Phase-Phase to ground Line Fault at 49ms, Z_f= 5 Ω

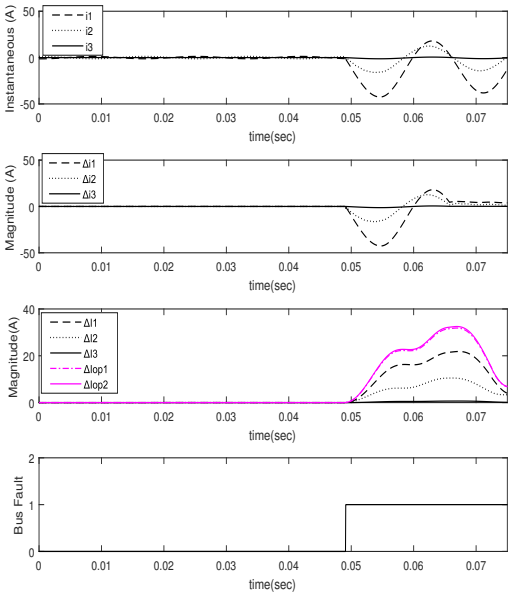

Figure A.30: Phase-Phase to ground Bus Fault at 49ms, Z_f= 0.1 Ω

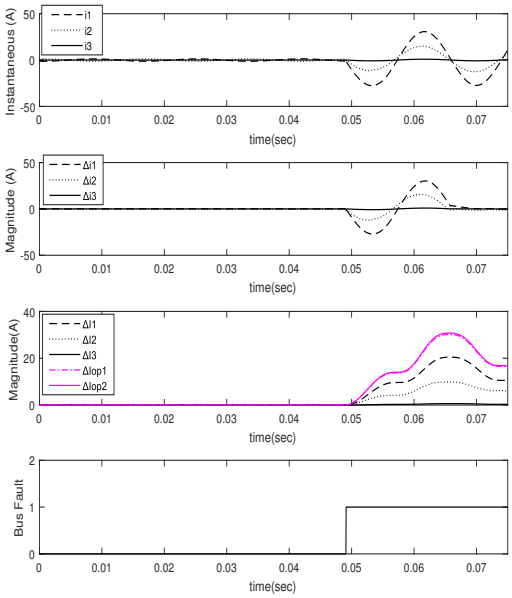

Figure A.31: Phase-Phase to ground Bus Fault at 49ms, Z_f= 5 Ω

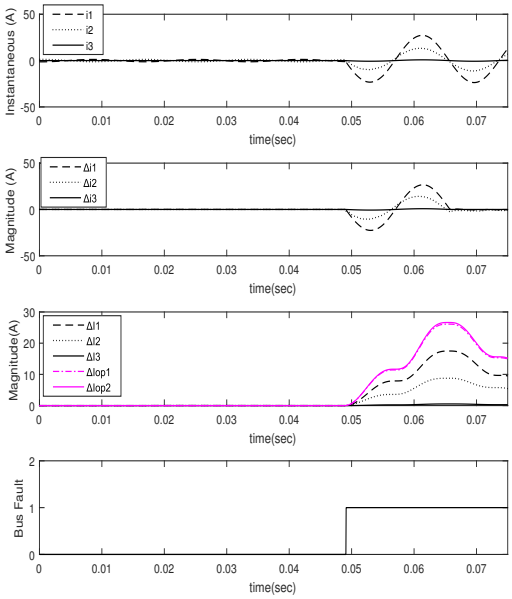

Figure A.32: Phase-Phase to ground Bus Fault at 49ms, Z_f= 10 Ω

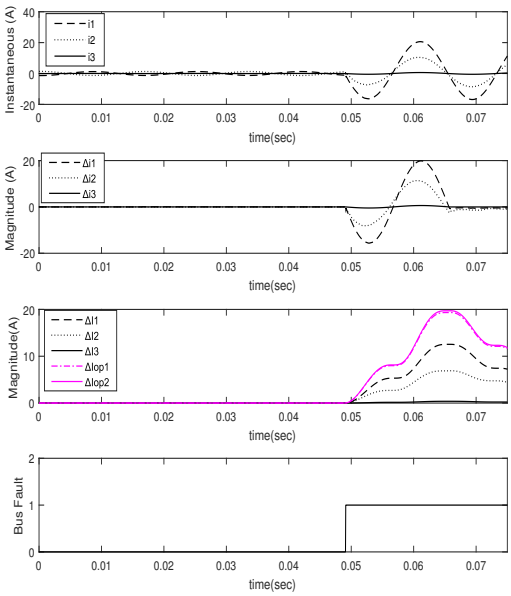

Figure A.33: Phase-Phase Bus Fault at 49ms, Z_f= 0.1 Ω

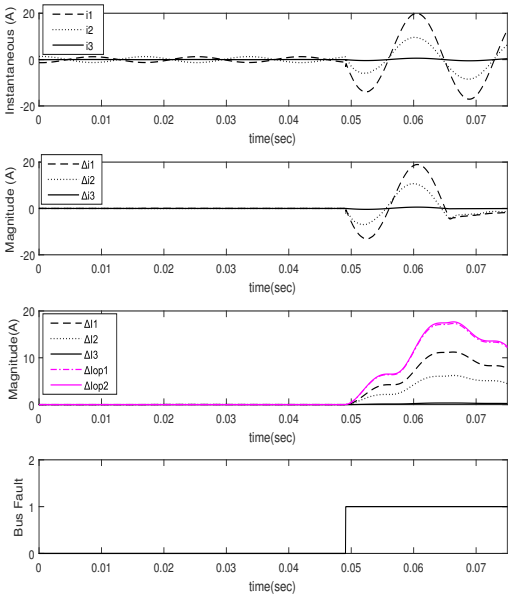

Figure A.34: Phase-Phase Bus Fault at 49ms, Z_f= 5 Ω

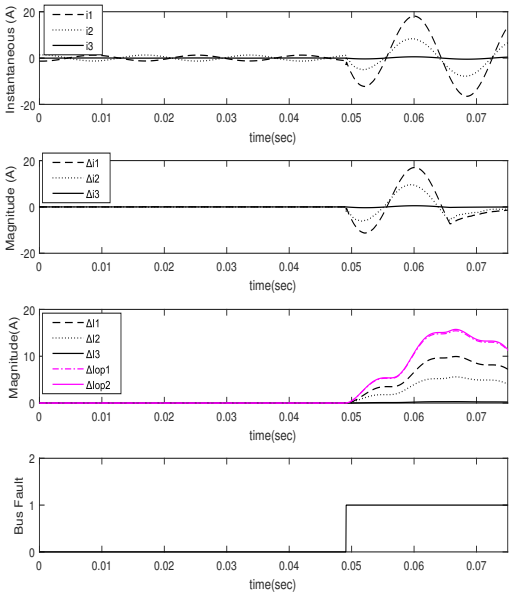

Figure A.35: Phase-Phase Bus Fault at 49ms, Z_f= 10 Ω

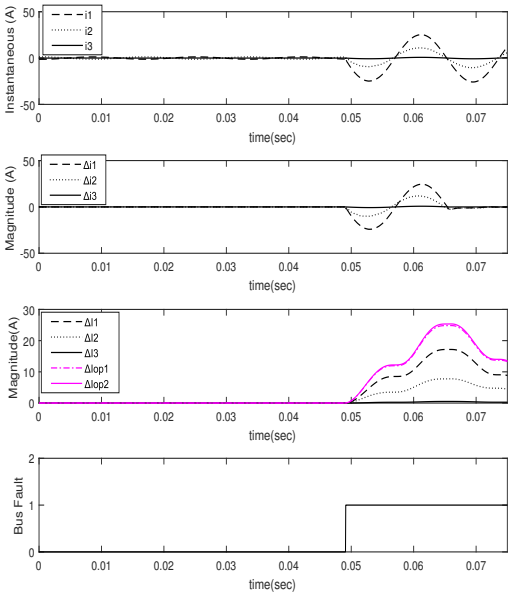

Figure A.37: Phase to ground Bus Fault at 49ms, Z_f= 5 Ω

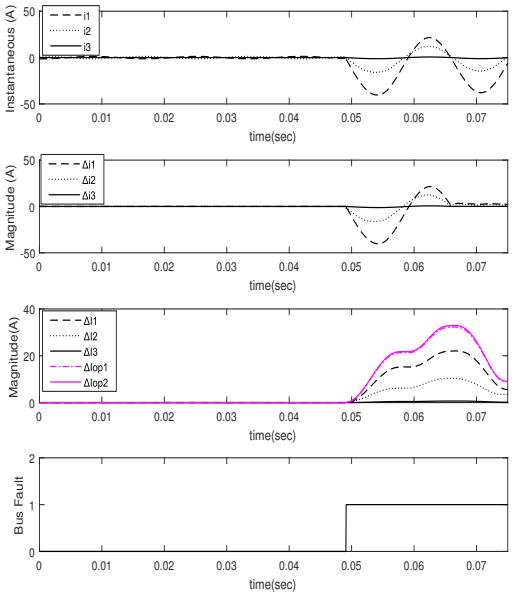

Figure A.36: Phase to ground Bus Fault at 49ms, Z_f= 0.1 Ω

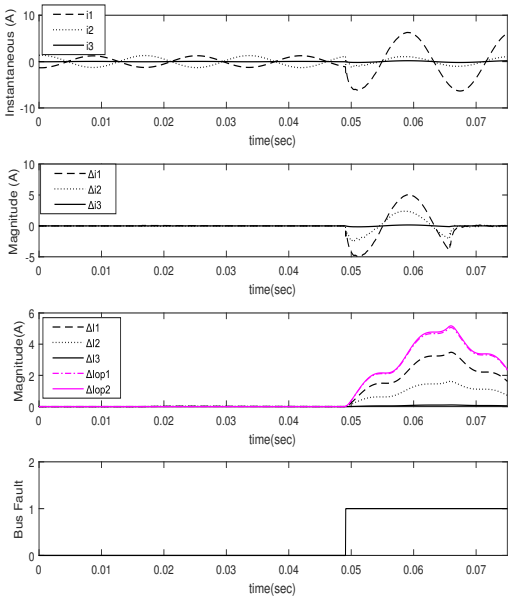

Figure A.38: Phase to ground Bus Fault at 49ms, Z_f= 50 Ω

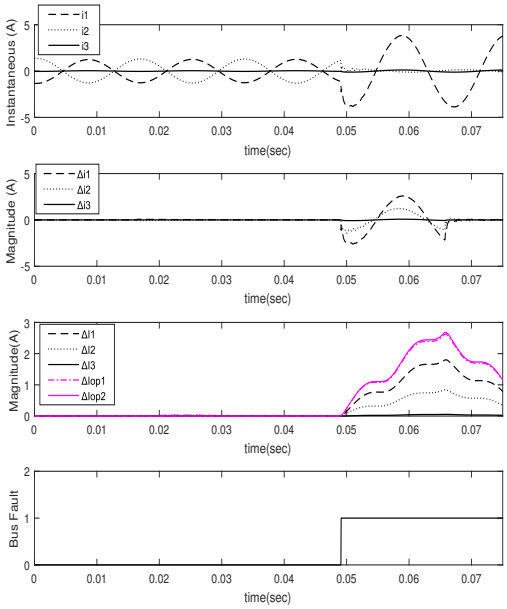

Figure A.39: Phase to ground Bus Fault at 49ms, Z_f= 100 Ω

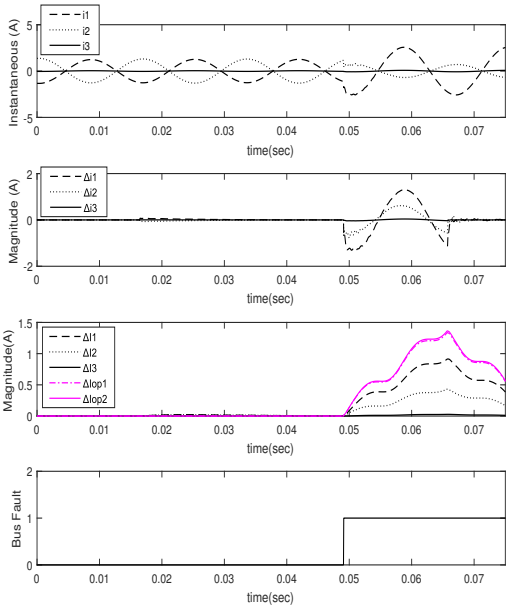

Figure A.40: Phase to ground Bus Fault at 49ms, Z_f= 200 Ω

A.3 Matlab code for 4-bus Test System


```
w=2*pi*60;
for i = 1:1:(length(Xaxis)-2)%taking out first two values
    Xaxisr(i)= Xaxis(i+2);
    m1r(i)= m1(i+2);
    m2r(i)= m2(i+2);
    m3r(i)= m3(i+2);
    m4r(i)= m4(i+2);
end
for i = 1:1:length(m1r)%to subtract t with t-T
    if i<=200
      m1n(i)= 0;
      m2n(i)= 0;
      m3n(i)= 0;
      m4n(i)= 0;
    else
   Xaxisa= Xaxisr(i)-0.0167;
   for a= 1:1:length(Xaxisr)
   if Xaxisr(a) >= Xaxisa
      m1n(i)= m1r(i)-m1r(a);
      m2n(i)= m2r(i)-m2r(a);
      m3n(i)= m3r(i)-m3r(a);
      m4n(i)= m4r(i)-m4r(a);
      break
   end
 end
    end
end
N=200;
r=1;
while r<=length(m1r)
%while r<=2
mc1(r)=0;ms1(r)=0;mc2(r)=0;ms2(r)=0;mc3(r)=0;ms3(r)=0;mc4(r)=0;ms4(r)=0;
for i=(-199+r:1:r)
    if i<=0
        mc1(r)=0;
        ms1(r)=0;
        mc2(r)=0;
        ms2(r)=0;
        mc3(r)=0;
        ms3(r)=0;
        mc4(r)=0;
        ms4(r)=0;
    else
        mc1(r)= mc1(r)+m1n(i)*cos(w*Xaxisr(i));
        ms1(r)= ms1(r)+m1n(i)*sin(w*Xaxisr(i));
        mc2(r)= mc2(r)+m2n(i)*cos(w*Xaxisr(i));
        ms2(r)= ms2(r)+m2n(i)*sin(w*Xaxisr(i));
        mc3(r)= mc3(r)+m3n(i)*cos(w*Xaxisr(i));
        ms3(r)= ms3(r)+m3n(i)*sin(w*Xaxisr(i));
        mc4(r)= mc4(r)+m4n(i)*cos(w*Xaxisr(i));
        ms4(r)= ms4(r)+m4n(i)*sin(w*Xaxisr(i));
```

```
    end
end
Irms1(r)= (1/((N/2)*sqrt(2)))*sqrt(mc1(r)^2+ms1(r)^2);
Phase1(r)=atan2(ms1(r),mc1(r))*(180/pi);
Irms2(r)= (1/((N/2)*sqrt(2)))*sqrt(mc2(r)^2+ms2(r)^2);
Phase2(r)=atan2(ms2(r),mc2(r))*(180/pi);
Irms3(r)= (1/((N/2)*sqrt(2)))*sqrt(mc3(r)^2+ms3(r)^2);
Phase3(r)=atan2(ms3(r),mc3(r))*(180/pi);
Irms4(r)= (1/((N/2)*sqrt(2)))*sqrt(mc4(r)^2+ms4(r)^2);
Phase4(r)=atan2(ms4(r),mc4(r))*(180/pi);
r=r+1;
end
for i=1:1:length(m1r)
    Recx1(i)= Irms1(i)*cos((pi/180)*Phase1(i));
    Recy1(i)= Irms1(i)*sin((pi/180)*Phase1(i));
    Z1(i)= complex(Recx1(i),Recy1(i));
    Recx2(i)= Irms2(i)*cos((pi/180)*Phase2(i));
    Recy2(i)= Irms2(i)*sin((pi/180)*Phase2(i));
    Z2(i)= complex(Recx2(i),Recy2(i));
    Recx3(i)= Irms3(i)*cos((pi/180)*Phase3(i));
    Recy3(i)= Irms3(i)*sin((pi/180)*Phase3(i));
    Z3(i)= complex(Recx3(i),Recy3(i));
    Recx4(i)= Irms4(i)*cos((pi/180)*Phase4(i));
    Recy4(i)= Irms4(i)*sin((pi/180)*Phase4(i));
    Z4(i)= complex(Recx4(i),Recy4(i));
    Iop1(i)= Z1(i)+Z2(i);
    Iop2(i)= Iop1(i)+Z3(i);
    Iop3(i)= Iop2(i)+Z4(i);
    MIop1(i) = abs(Iop1(i));
    AIop1(i)= angle(Iop1(i))*(180/pi);
    MIop2(i) = abs(Iop2(i));
    AIop2(i)= angle(Iop2(i))*(180/pi);
    MIop3(i) = abs(Iop3(i));
    AIop3(i)= angle(Iop3(i))*(180/pi);
 end
for i= 1:1:length(m1r)
  if MIop1(i)>Irms1(i) && MIop1(i)>Irms2(i)
      if MIop2(i)>(MIop1(i)-0) && MIop2(i)>(Irms3(i))
          if MIop3(i)>(MIop2(i)) && MIop3(i)>Irms4(i)
                        Fault(i)=1;
          else
              Fault(i)=0;
          end
      else
          Fault(i)=0;
      end
  else
      Fault(i)=0;
  end

end
```

A.4 Matlab code for IEEE 14-bus Test System


```
w=2*pi*60;
for i = 1:1:(length(Xaxis)-2)%taking out first two values
    Xaxisr(i)= Xaxis(i+2);
    m1r(i)= ct1(i+2);
    m2r(i)= ct2(i+2);
    m3r(i)= ct3(i+2);
end
for i = 1:1:length(m1r)%to subtract t with t-T
    if i<=200
      m1n(i)= 0;
      m2n(i)= 0;
      m3n(i)= 0;
    else
   Xaxisa= Xaxisr(i)-0.0167;
   for a= 1:1:length(Xaxisr)
   if Xaxisr(a) >= Xaxisa
      m1n(i)= m1r(i)-m1r(a);
      m2n(i)= m2r(i)-m2r(a);
      m3n(i)= m3r(i)-m3r(a);
      break
   end
 end
    end
end
N=200;
r=1;
while r<=length(m1r)
mc1(r)=0;ms1(r)=0;mc2(r)=0;ms2(r)=0;mc3(r)=0;ms3(r)=0;
for i=(-199+r:1:r)
    if i<=0
        mc1(r)=0;
        ms1(r)=0;
        mc2(r)=0;
        ms2(r)=0;
        mc3(r)=0;
        ms3(r)=0;

    else
        mc1(r)= mc1(r)+m1n(i)*cos(w*Xaxisr(i));
        ms1(r)= ms1(r)+m1n(i)*sin(w*Xaxisr(i));
        mc2(r)= mc2(r)+m2n(i)*cos(w*Xaxisr(i));
        ms2(r)= ms2(r)+m2n(i)*sin(w*Xaxisr(i));
        mc3(r)= mc3(r)+m3n(i)*cos(w*Xaxisr(i));
        ms3(r)= ms3(r)+m3n(i)*sin(w*Xaxisr(i));

    end
end
Irms1(r)= (1/((N/2)*sqrt(2)))*sqrt(mc1(r)^2+ms1(r)^2);
Phase1(r)=atan2(ms1(r),mc1(r))*(180/pi);
Irms2(r)= (1/((N/2)*sqrt(2)))*sqrt(mc2(r)^2+ms2(r)^2);
Phase2(r)=atan2(ms2(r),mc2(r))*(180/pi);
```

```
Irms3(r)= (1/((N/2)*sqrt(2)))*sqrt(mc3(r)^2+ms3(r)^2);
Phase3(r)=atan2(ms3(r),mc3(r))*(180/pi);
r=r+1;
end
for i=1:1:length(m1r)
    Recx1(i)= Irms1(i)*cos((pi/180)*Phase1(i));
    Recy1(i)= Irms1(i)*sin((pi/180)*Phase1(i));
    Z1(i)= complex(Recx1(i),Recy1(i));
    Recx2(i)= Irms2(i)*cos((pi/180)*Phase2(i));
    Recy2(i)= Irms2(i)*sin((pi/180)*Phase2(i));
    Z2(i)= complex(Recx2(i),Recy2(i));
    Recx3(i)= Irms3(i)*cos((pi/180)*Phase3(i));
    Recy3(i)= Irms3(i)*sin((pi/180)*Phase3(i));
    Z3(i)= complex(Recx3(i),Recy3(i));
    Iop1(i)= Z1(i)+Z2(i);
    Iop2(i)= Iop1(i)+Z3(i);
    MIop1(i) = abs(Iop1(i));
    AIop1(i)= angle(Iop1(i))*(180/pi);
    MIop2(i) = abs(Iop2(i));
    AIop2(i)= angle(Iop2(i))*(180/pi);
end
for i= 1:1:length(m1r)
  if MIop1(i)>Irms1(i) && MIop1(i)>Irms2(i)
      if MIop2(i)>(MIop1(i)-0) && MIop2(i)>(Irms3(i))
                           Fault(i)=1;

      else
          Fault(i)=0;
      end
  else
      Fault(i)=0;
  end
end
```

Vita

Bishwas Baral is an Electrical Engineering Masters student at the University of New Orleans, LA, USA. He received his Bachelor Degree in Electrical Engineering from Tribhuvan University, Nepal. He is currently working as a graduate research assistant with Dr. Parviz Rastgoufard and Dr. Ittiphong Leevongwat in UNO-Entergy Power and Energy Research Lab (PERL). His research areas include power system planning, modeling, simulation, protection, and energy management.